SIMULATION OF A DIAPHRAGM TYPE FLUID OSCILLATOR

by

Seshadri Sankar

A RESEARCH THESIS

IN THE

FACULTY OF ENGINEERING

Presented in partial fulfilment of the requirements

for the

Degree of MASTER OF ENGINEERING

at

Sir George Williams University

Montreal, Canada

11th August, 1971

ABSTRACT

A mathematical model of a diaphragm fluid oscillator is presented. The formulation of the system equations is carried out using linear graph methods. The solutions of the dynamic equations are obtained by digital computer simulation using numerical techniques. Experimental measurements are carried out on a prototype oscillator and the experimental results obtained are described and compared with the predicted theoretical results.

The theoretical results give the frequency of oscillation, the pressure fluctuations in the two chambers and the displacement of the diaphragm for all instants of time. Both the theoretical analysis and the experimental results show that the main operating principle of this oscillator is the inertial effect of the fluid in the vent tube. Accordingly, the frequency of oscillation is directly proportional to the cross-sectional area of the vent tube and inversely proportional to the length of the tube. The effect of various parameters affecting the frequency of oscillation are considered and studied.

ACKNOWLEDGEMENTS

The author expresses his profound gratitude to his thesis supervisor, Dr. G.S. Mueller, for his valuable guidance and encouragement at all times. The author also wishes to express his gratitude to Dr. C.K. Kwok for suggesting the problem and the help extended during the investigation.

Finally, the author acknowledges the help of the National Research Council of Canada for financial support from Research Grant No. A7436.

TABLE OF CONTENTS

LIST OF FIGURES

LIST OF TABLES

NOMENCLATURE

A	cross-sectional area (in^2)
C_d	coefficient of discharge
D	diameter of seat chamber (in)
F	force due to pressure (lb)
F_k	force due to spring (lb)
F_m	force due to inertia of diaphragm (lb)
g	acceleration due to gravity (in/sec^2)
I	fluid inertance in vent tube ($lb\text{-}sec^2/in^5$)
k	spring stiffness (lb/in)
L	length of vent tube (in)
M	lumped mass of diaphragm (slugs)
P	pressure (psig)
P_s	supply pressure (psig)
Q	volume flow rate of fluid (in^3)
R	fluid resistance ($lb\text{-}sec/in^5$)
v	velocity of fluid (in/sec)
y	displacement of diaphragm from seat (in)
y_{max}	maximum displacement of diaphragm (in)
$\dot{y}$	velocity of diaphragm (in/sec)
ν	specific weight of fluid (lb/in^3)
ρ	density of fluid ($slug/in^3$)

<u>subscripts</u>

1	seat chamber
2	vent chamber

n	supply nozzle
o	output orifice
S	curtain area
v	vent tube

CHAPTER 1

INTRODUCTION

1.1 Background

The recent trend in hydraulic and pneumatic control systems is the use of discontinuous on-off type controls rather than the conventional linear continuous control. Such on-off control systems usually consist of a form of pulse modulation or bang-bang optimal switching. One of the key elements in a pulsed system is a clock that either generates the pulses or determines when they are going to occur. The clock function is usually performed by an oscillator. A pneumatic oscillator is ideally suited for a pneumatic pulse length modulated system[1]. Fluidic oscillators are also used in analog fluidic systems as frequency modulators[2].

Fluidic oscillators have also found increasing applications for sensing and analog to digital converter purposes. Such fluidic oscillators are made of a monostable or a bistable fluidic amplifier with some form of feedback[3].

Sensing can be performed with an oscillator in two ways. First, an oscillator construction feature, such as the feedback capacitance, can be changed by the measured quantity. An example of such an application is a liquid level sensor. A change in the liquid level generates a frequency change in the oscillator, proportional to the level[4]. Second, if a fluid variable such as temperature or density is to be measured, the fluid can be passed through the oscillator and the frequency change will give a measure of the variable[5,6].

These oscillators are made of some fluidic elements, use air as the medium and operate at higher frequencies. Very little work has been done on liquid operated, low frequency oscillators. This thesis presents the dynamic behaviour of a low frequency liquid operated oscillator with a minimum of moving parts.

1.2 Description of the Fluid Oscillator

A schematic cross-sectional view of the fluid oscillator is shown in Fig. 1. The fluid oscillator consists of a supply nozzle which directs the flow into a receiver. The receiver has a larger diameter than the supply nozzle and is located concentric with the supply nozzle. Between the receiver and the supply nozzle there is a small gap which is termed the ejector chamber. This ejector chamber is connected to the output line. The unit with supply nozzle, receiver and the output line acts as an ejector system. The other end of the receiver connects to the seat chamber. Surrounding the seat chamber is the vent chamber together with a vent tube. A diaphragm made of polyurethane sits on the seat and closes the curtain area between the two chambers. A spring with a force-adjusting screw is provided to keep the diaphragm in position. A spring retainer is placed between the diaphragm and the spring to make the motion of the diaph-

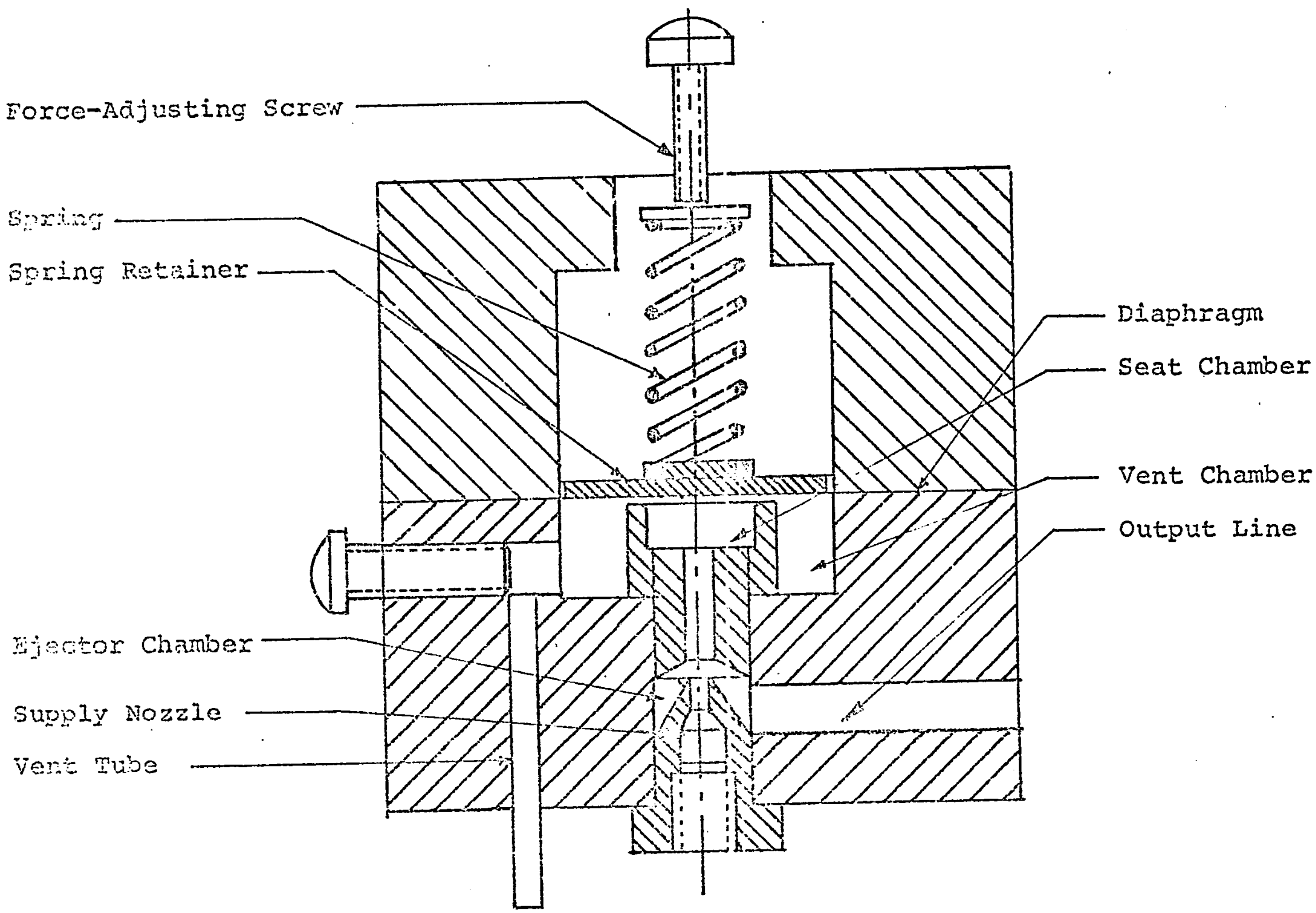

FIG. 1. SCHEMATIC CROSS-SECTIONAL VIEW OF FLUID OSCILLATOR.

ragm uniform.

1.3 Operating Principle

Fluid at a supply pressure P_s is fed through the supply nozzle A_n into the seat chamber where pressure is P_1. The initial spring force causes the diaphragm to sit on the seat and closes the curtain area. Hence there will not be any flow into the vent chamber. As the pressure P_1 in the seat chamber builds up, the diaphragm starts to move up and allows flow into the vent chamber where pressure is P_2. This upward movement of the diaphragm will cause the pressure P_1 to decrease and the pressure P_2 to increase. The diaphragm movement is upwards as long as the force exerted due to the pressures P_1 and P_2, as well as inertial forces due to diaphragm mass, is more than the downward force of the spring. When the spring force overcomes the total upward forces, the diaphragm starts to move down, increasing P_1 and decreasing P_2.

Consider the situation when the diaphragm has moved down and closes the curtain area. At this instant the supply flow is continuously entering the supply nozzle and the flow passage to the vent chamber is completely blocked. Hence there will be flow through the outlet passage, accelerating the whole volume of the fluid in that passage. This creates the output to attain an instantaneous pressure which is higher than that of the supply pressure. However, at the same time the pressure P_2 in the vent chamber causes the flow out through the vent tube. But since there is no flow into the vent chamber and the outflow through the vent tube is continuous, a sub-ambient pressure results in the vent chamber. The flow through the vent tube is maintained because of the momentum of the fluid due to the pressure P_2 just before the diaphragm closes the seat. After a short interval of time, the momentum of the fluid in the vent tube is reduced to zero and the pressure in the vent chamber becomes atmospheric. Now the pressure P_1 in the seat chamber is high enough to push the diaphragm upwards against the spring force and starts the next cycle.

The inertial effect of the fluid in the vent tube is responsible for the oscillation phenomenon; hence the variation in the length and diameter of the vent tube will change the inertial effect and thus cause a change in the oscillation frequency.

1.4 Purpose and Scope of the Study

The purpose of this thesis is to mathematically model the fluid oscillator and to study the dynamic behaviour of this mechanism. In addition, the optimization of the parameters of the oscillator, for particular purposes, can be carried out. Experimental results are presented to compare with the theoretical results obtained.

The dynamic equations are obtained by considering a lumped parameter equivalent system. The solutions of the dynamic equations are obtained by digital computer simulation using numerical techniques. The solution gives the pressure fluctuations in the seat and vent chambers, the diaphragm displacement at different instants of time and the frequency of oscillation. The various parameters which affect the frequency and the pressure fluctuations are considered and studied.

CHAPTER 2

MATHEMATICAL ANALYSIS OF THE FLUID OSCILLATOR

2.1 General Remarks

In most fluid systems, the mathematical analysis is not done in a rigorous way because of the inherent difficulty in describing the system using differential equations. Usually, the analysis will be based on the experimental results obtained for the particular system. Either the experimental data or the characteristic curves drawn using the experimental data will be used in studying the performance of that system.

In most cases, even if the differential equation is known, it may be non-linear with time-varying parameters which introduce more difficulties in obtaining the solutions using classical methods. Using either numerical techniques with a digital computer or simulating on an analog computer will be the more realistic way of getting the solution.

2.2 Linear Graph Technique

A linear graph is a set of interconnected lines. A linear graph will be used first as an aid in visualizing the structure of the system and second as a basis for a general technique for formulating the system equations. The important advantage of the graph-theoretical models lies in that they lend themselves to a systematic procedure for the piece-wise solution of the problem.

The schematic representation of the linear graph for the fluid oscillator is shown in Fig. 2. The linear graph theory utilizes the sets of continuity equations and the terminal equations (component characteristics) as an integral part of the formulation procedure[7]. In other words, a set of non-linear and linear algebraic equations describing the system is generated through the following three sets of equations:

(i) Node - continuity equations,

(ii) Loop - compatibility equations,

(iii) Terminal or elemental equations.

2.3 Assumptions

(1) The fluid is considered to be incompressible.

(2) One dimensional, lumped parameter analysis is considered.

(3) The displacement of the diaphragm is in a straight line perpendicular to the supply nozzle.

(4) Velocity heads are considered to be negligible in comparison to the pressure head, except in the vent tube.

2.4 Description of the Linear Graph

In order to draw the linear graph, the fluid oscil-

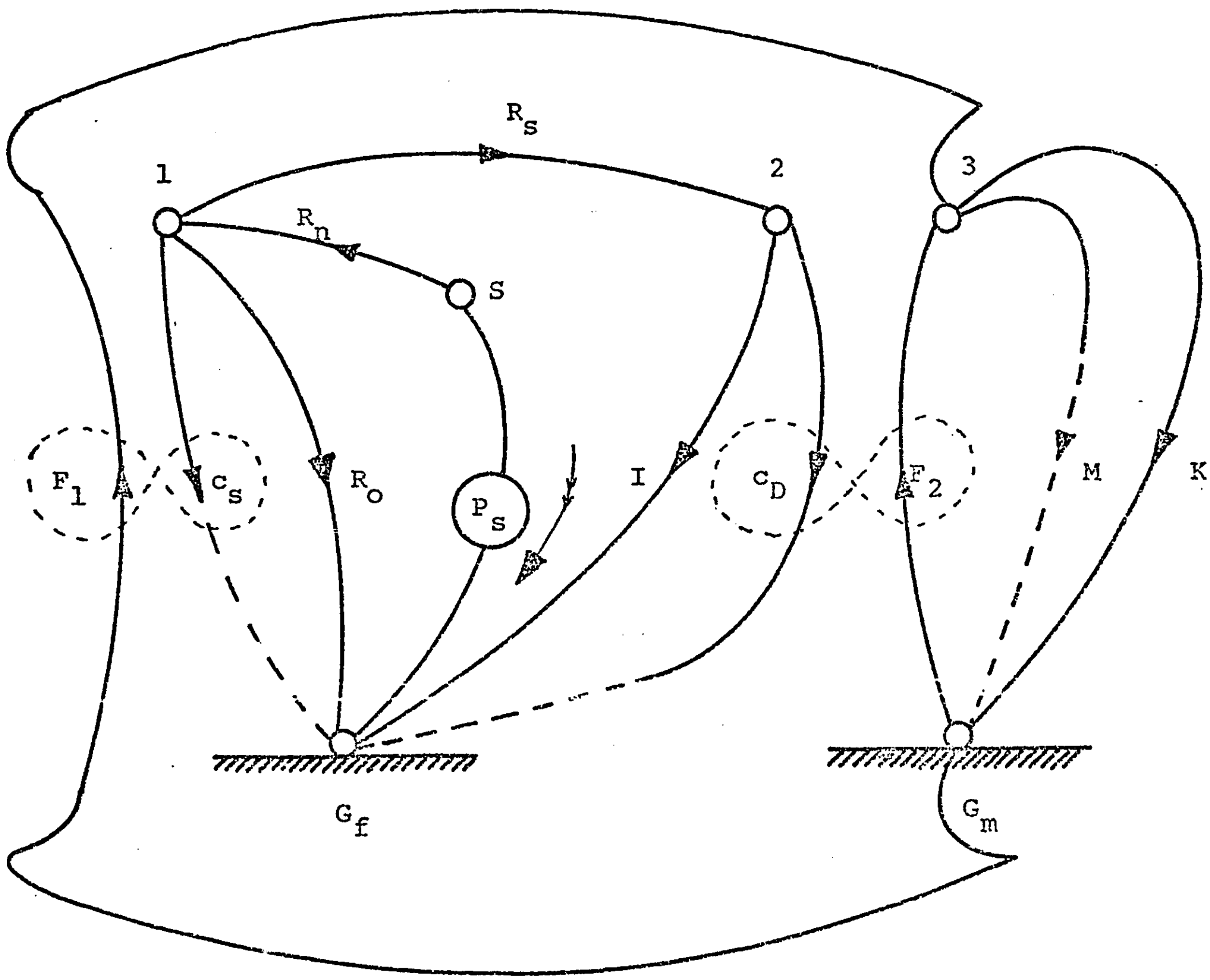

FIG. 2. LINEAR GRAPH OF FLUID OSCILLATOR.

lator can be considered as three separate systems:

1. The fluid system consisting of the supply nozzle, ejector system, seat chamber, vent chamber and vent tube,

2. The mechanical system consisting of the spring and a mass (lumped mass of the diaphragm and the spring retainer),

3. The linkage between the above two systems.

In the fluid system, pressure acts as an across-variable and the flow as a through-variable. The supply pressure P_s acts as the source. This is represented in the system graph between the vertex S and the fluid ground G_f. The flow through the supply nozzle is represented by the path S1. The vertex 1 indicates the lumped pressure P_1 in the seat chamber. The path 12 represents the variable resistance over the curtain area between the seat chamber and the diaphragm. The path $2G_f$ is the flow through the vent tube which represents the inertance of the fluid in that tube.

In the case of the mechanical system, velocity acts as an across-variable and the force as a through-variable. In the linear graph, mass and spring are connected in parallel between the vertices 3 and the mechanical ground G_m. The vertex 3 represents the velocity of the diaphragm. The connections between the two above systems are represented by the set of paths $2G_f$, $3G_m$ and $1G_f$, $3G_m$ as shown in Fig. 2. The linkage is represented by a pure gyrating transducer which transforms an across-variable into a through-variable and changes a through-variable into an across-variable between two types of systems. The dashed reverse loop in the linear graph represents the gyration. There are two gyrating transducers associated with the system, each one connecting the mechanical system to one of the two chambers. The arrows associated with the system graph represent positive direction of through-variable flow and positive direction of across-variable drop.

2.5 Formulation of the System Equations

To formulate the system equations, the following set of equations may be used.

(i) Node - continuity equations,

(ii) Path - compatibility equations,

(iii) Elemental equations.

For a linear or non-linear system, this set of equations is sufficient to determine the system performance. For non-linear systems, it may not be possible to eliminate all but one variable since it may involve transcendental relations between some or all variables and hence the whole set may have to be treated simultaneously.

Now consider the fluid system and apply continuity conditions at each vertex. The continuity condition at the vertex is often called the vertex law and is essentially applying the principle of conservation of matter or force.

At vertex S,

$$Q_S = Q_{R1} \tag{2.1}$$

where Q_S and Q_{R1} are the volume rates of flow (in^3/sec) from the supply and through the supply nozzle.

At vertex 1,

$$Q_1 + Q_{RO} + Q_{RS} - Q_{R1} = 0 \tag{2.2}$$

where Q_1, Q_{RO} and Q_{RS} are the volume flow rate through the seat chamber, outlet and curtain area, respectively.

At vertex 2,

$$Q_I + Q_2 - Q_{RS} = 0 \tag{2.3}$$

where Q_I and Q_2 are the volume flow rate through the vent tube and vent chamber.

The elemental equations connecting the through-variables and the across-variables may be written as:

$$P_s - P_1 = R_n(P_s, P_1)Q_{R1} \tag{2.4}$$

$$P_1 = R_O(P_1)Q_{RO} \tag{2.5}$$

$$P_1 - P_2 = R_s(P_1, P_2)Q_{RS} \tag{2.6}$$

$$P_2 = I \frac{dQ_I}{dt} \tag{2.7}$$

where $R_n(P_s, P_1)$, $R_0(P_1)$ and $R_s(P_1, P_2)$ are the non-linear fluid resistances and the derivation of which are shown in Appendix I

P_s is the supply pressure (psig)

P_1 and P_2 are the pressures in seat and vent chambers (psig)

I is the fluid inertance of the vent tube given by $\rho L/A_v$

where ρ is the density of the fluid, L is the length of the vent tube, A_v is the cross-sectional area of the vent tube.

The gyrator action is generated by the two sets of loops in the linear graph shown in Fig. 2. The gyrator relationship can be obtained by writing the relationship between the across-variable and the through-variable for each loop concerned. They can be written as:

$$\dot{y} = \frac{1}{A_1} Q_1 \tag{2.8}$$

$$F_1 = A_1 P_1 \tag{2.9}$$

$$\dot{y} = \frac{1}{A_2} Q_2 \tag{2.10}$$

$$F_2 = A_2 P_2 \tag{2.11}$$

where $\dot{y}$ is the velocity of the diaphragm (in/sec)

F_1 and F_2 are the forces due to P_1 and P_2 acting on the diaphragm (lb)

A_1 and A_2 are cross-sectional areas of the seat and vent chambers (in^2).

The equations concerned with the mechanical system are the dynamic force balance of the diaphragm and the individual elemental equations. They can be formulated as:

$$F_1 + F_2 - F_m - F_k = 0 \qquad (2.12)$$

$$F_m = m \frac{d\dot{y}}{dt} \qquad (2.13)$$

$$\dot{y} = \frac{1}{k} \frac{dF_k}{dt} \qquad (2.14)$$

where F_m and F_k are the inertial and spring forces (lb)

m is the lumped mass of the mechanical system (slugs)

k is the spring stiffness (lb/in).

2.6 Simulation Procedure

The set of 14 equations shown in Section (2.5) are sufficient to describe the system completely within the major assumptions. Equations (2.4), (2.5) and (2.6) are non-linear whereas all other equations are linear. Solutions of this set are possible only through a digital computer or through analog computer simulation. In this thesis, simulation is carried out by digital computer using a Runge-Kutta integration method. The procedure is explained in the succeeding paragraphs.

The system equations consist of three differential equations connecting the independent variable time (t) and the dependent variables Q_I, $\dot{y}$ and F_k. Obviously, three initial conditions, $Q_I(0)$, $\dot{y}(0)$ and $F_k(0)$ are needed to solve these differential equations. Hence the first step in the simulation procedure is to get the proper initial conditions. Once these initial conditions are known, the following procedure may be adopted to obtain the solutions of the whole set.

Using equations (2.8) and (2.10), the values of Q_1 and Q_2 can be calculated as,

$$Q_1 = A_1\dot{y} \qquad (2.15)$$

$$Q_2 = A_2\dot{y} \qquad (2.16)$$

Substituting for Q_2 and Q_I in equation (2.3) gives

$$Q_{RS} = Q_I + Q_2 \qquad (2.17)$$

Substituting equation (2.17) into equation (2.2) gives

$$Q_{RO} - Q_{R1} = -\left[Q_1 + Q_{RS}\right] \qquad (2.18)$$

Using the values of the functions $R_n(P_s,P_1)$, $R_O(P_1)$ and $R_s(P_1,P_2)$ from Appendix I and rearranging equations (2.4), (2.5) and (2.6) gives

$$(P_s - P_1)^{1/2} = \frac{1}{c_d A_n (\frac{2}{\rho})^{1/2}} Q_{R1} \qquad (2.19)$$

$$P_1^{1/2} = \frac{1}{c_d A_o (\frac{2}{\rho})^{1/2}} Q_{RO} \qquad (2.20)$$

$$(P_1 - P_2)^{1/2} = \frac{1}{c_d \pi D y (\frac{2}{\rho})^{1/2}} Q_{RS} \qquad (2.21)$$

where c_d is the discharge coefficient

D is the diameter of the seat (in)

ρ is the density of the fluid (slugs/in^3)

y is the displacement of the diaphragm from the seat (in).

Rewriting equations (2.19), (2.20) and (2.21) gives,

$$P_s - P_1 = \frac{\rho}{2(c_d A_n)^2} \left|Q_{R1}\right| Q_{R1} \qquad (2.22)$$

$$P_1 = \frac{\rho}{2(c_d A_o)^2} \left|Q_{RO}\right| Q_{RO} \qquad (2.23)$$

$$P_1 - P_2 = \frac{\rho}{2(c_d \pi D y)^2} \left|Q_{RS}\right| Q_{RS} \qquad (2.24)$$

Consider equations (2.18), (2.22) and (2.23).

These are three algebraic equations with three unknown variables P_1, Q_{R1} and Q_{RO}. The variables can be found by solving the simultaneous equations. The procedure is outlined as follows:

$$\text{Let } c_1 = \frac{\rho}{2(c_d A_n)^2}$$

$$c_2 = \frac{\rho}{2(c_d A_o)^2}$$

$$c_3 = \frac{\rho}{2[c_d\ Dy]^2}$$

Substituting equation (2.23) in (2.22) and rearranging gives,

$$P_s = c_1|Q_{R1}|Q_{R1} + c_2|Q_{RO}|Q_{RO} \tag{2.25}$$

From equation (2.18)

$$Q_{R1} = Q_{RO} + [Q_1 + Q_{RS}]$$

Let $Q = Q_1 + Q_{RS}$

Therefore $$Q_{R1} = Q_{RO} + Q \tag{2.26}$$

Substituting the value of Q_{R1} from equation (2.26) in equation (2.25) gives,

$$P_s = c_1 \left|(Q + Q_{RO})\right| (Q + Q_{RO}) + c_2 \left|Q_{RO}\right| Q_{RO} \qquad (2.27)$$

The volume flow rate through the outlet Q_{RO} is always a positive quantity and hence the equation (2.27) can be written as,

$$P_s = c_1 \ \text{sign}(Q + Q_{RO})(Q + Q_{RO})^2 + c_2 \ Q_{RO}^2 \qquad (2.28)$$

Rearranging equation (2.28) gives,

$$Q_{RO}^2 + \frac{2\bar{c}_1 Q}{(c_2 + \bar{c}_1)} Q_{RO} + \frac{\bar{c}_1 Q^2 - P_s}{(c_2 + \bar{c}_1)} = 0 \qquad (2.29)$$

where $\bar{c}_1 = c_1 \ \text{sign}(Q + Q_{RO})$.

$\bar{c}_1$ can have only two values. That is

$$\bar{c}_1 = c_1$$

$$\text{or} \quad \bar{c}_1 = -c_1$$

Hence the equation (2.29) will have four solutions for Q_{RO}. Since the physical system is deterministic, there can exist only one admissible value for Q_{RO}. In order to find the proper value of Q_{RO}, a certain constraint on Q_{RO} must be satisfied. This constraint can be established by analyzing the maximum and minimum of Q_{RO}. The volume rate of flow through the outlet, Q_{RO}, is maximum when the pressure P_1 in the seat chamber is maximum, and vice versa. The pressure P_1 always lies between the range zero and the supply pressure

P_s. Hence the outflow Q_{RO} ranges between zero and a maximum value for Q_{RO}. Mathematically, this constraint on Q_{RO} can be expressed as

$$0 \leq Q_{RO} \leq (Q_{RO})_{max} \tag{2.30}$$

where

$$(Q_{RO})_{max} = \left[\frac{(P_1)_{max}}{c_2}\right]^{1/2}$$

$$= \left(\frac{P_s}{c_2}\right)^{1/2}$$

Thus the value for Q_{RO} can be determined from the solution of equation (2.29) and the constraint (2.30).

Substituting the value of Q_{RO} in equation (2.23), the pressure P_1 can be calculated as,

$$P_1 = c_1 Q_{RO}^2 \tag{2.31}$$

Using the value of P_1 and substituting in equation (2.24) gives,

$$P_2 = P_1 - c_3 |Q_{RS}| Q_{RS} \tag{2.32}$$

Substituting equations (2.31) and (2.32) in equations (2.9) and (2.11) gives,

$$F_1 = A_1 P_1 \tag{2.33}$$

$$F_2 = A_2 P_2 \tag{2.34}$$

From the above two equations and using equation (2.12), the value of F_m can be calculated as,

$$F_m = F_1 + F_2 - F_k \tag{2.35}$$

Now the integrand of the three differential equations are known and hence the solution can be calculated using the Runge-Kutta method as explained in Appendix II. The whole cycle is repeated as the values of the pressures P_1, P_2 and the diaphragm displacement y at different instants can be calculated. The constants used in the fluid oscillator simulation are given in Appendix III.

The solution of one of the system differential equations gives the value of the volume flow rate through the vent tube when the diaphragm does not close the curtain area. The fluid motion in the vent tube is entirely different when the diaphragm closes the curtain area and the equations concerning this fluid motion are discussed in Appendix IV.

CHAPTER 3

EXPERIMENTAL WORK

3.1 Introduction

In order to verify the theory developed for the fluid oscillator, experimental work has been carried out using a prototype oscillator*. A pictorial view of the oscillator with its components is shown in Fig. 3. The construction of the oscillator is very similar to that of the schematic shown in Fig. 1. Provision is made in the oscillator for fixing various vent tubes of different lengths and diameters. The experimental work carried out fulfilled two distinct purposes. In the first case, it gives qualitative information on the frequency of oscillation and the output pressure for different lengths and diameters of the vent tube. Secondly, it allows experiment to show the effect of initial spring force and supply pressure on the frequency of oscillation.

The experiments are carried out using only one prototype oscillator with different vent tubes. These experiments are done only for blocked output condition. The pressure fluctuations and the oscillation frequencies are measured by an oscilloscope through a pressure transducer. The recordings are carried out using an oscilloscope camera.

Designed by Dr. C.K. Kwok of the Fluid Controls Group at Sir George Williams University.

FIG. 3 PROTOTYPE OSCILLATOR

3.2 Experimental Apparatus

The general set-up of the experimental apparatus is shown in Fig. 4. This consists of the fluid oscillator with all its components connected to the supply line and the measurement unit. The measurement unit consists of a pressure transducer, an oscilloscope and an oscilloscope camera. The supply to the fluid oscillator is from the water main through a regulator.

Because of the small size of the device, all measurements are taken at the entrance and exit of the oscillator. Since the measurements are made with a pressure transducer, the question of frequency response of the transducer arises. The situation wherein a liquid is being used in a transducer is entirely different from that of a gas-filled apparatus. A liquid is characterized by a high density and stiffness, while a gas at ordinary pressure has a density and stiffness several orders lower in magnitude than a liquid. This causes a transducer, comprising a mass, suspended by a spring, to change its natural frequency as soon as it is charged with a liquid[8]. This indicates that the length of tubing, connecting the oscillator and the transducer has an effect in changing the natural frequency of the transducer and thereby affecting the result of the oscillator output. Hence it is desirable to have the measuring equipment as close to the system as possible to eliminate the undesirable effects caused by interconnecting tubing.

FIG. 4 EXPERIMENTAL APPARATUS

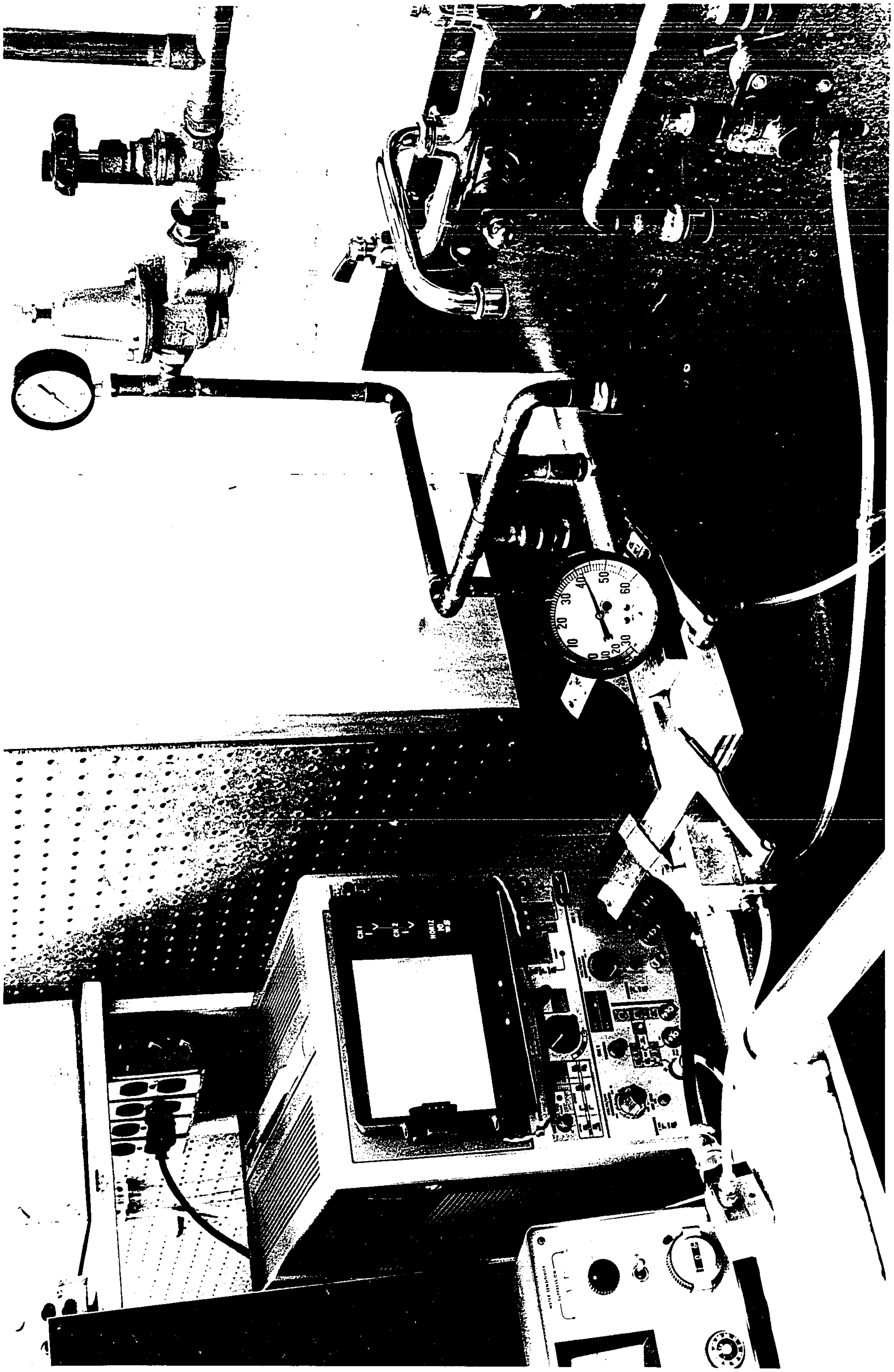

3.3 Procedure

The first step in the experimental work is to calibrate the pressure transducer. A suitable sensitivity of the transducer is selected and a known supply pressure level is applied. The transducer indicator is adjusted to the required reading. Now the supply pressure is cut off and the indicator is checked for zero reading. If it does not read zero, it is adjusted to do so. The process is repeated until the desired calibration of the transducer is arrived at. In the experimental apparatus, the transducer is calibrated to give 3 volts output for 40 psig of supply pressure.

Before applying supply pressure to the oscillator, the initial spring force is adjusted and kept at a constant value. A vent tube of known diameter and length is fitted into the vent chamber. All the measuring equipment is connected as explained above. Now a constant supply pressure is applied to the fluid oscillator. The oscillation of the fluid jet begins and the frequency of oscillation and the output pressure are measured on the oscilloscope. These outputs are also recorded using an oscilloscope camera. The experiment is repeated using different lengths and diameters of vent tube. The vent tubes used are made of brass and have lengths between 6 and 12 inches and diameters between 4/32 and 7/32 inch.

To study the effect of supply pressure and initial spring force on the oscillation frequency, experiments are carried out with different supply pressure and spring force. Supply pressures of 40 psig, 30 psig and 20 psig are used in the experiment.

CHAPTER 4

DISCUSSION OF RESULTS

4.1 Theoretical Analysis

The theoretical analysis developed for the fluid oscillator gives the dynamic equations of the system. These dynamic equations are developed using linear graph methods. This technique gives the system equations more easily and provides a systematic procedure for a piece-wise solution of the problem.

The results of the theoretical analysis give the position of the diaphragm and the pressures in the seat and vent chambers at different instants of time. A change in the vent tube geometry changes these pressure fluctuations and the diaphragm displacement. Figs. 5, 6 and 7 show the pressure fluctuations and the diaphragm displacement obtained from the theoretical analysis. The results of the analysis also show that the oscillation frequency is inversely proportional to the inertance of the vent tube. That is, the oscillation frequency is directly proportional to the cross-sectional area of the vent tube and inversely proportional to the length of the tube. Fig. 8 shows the effect of vent tube length and diameter on the oscillation frequency for a constant supply pressure.

The oscillation frequency depends on a number of variables such as the mass of the diaphragm, the diameter of the seat and vent chamber, the supply pressure, the spring stiffness, the initial spring force, and the diameter of the output orifice. The theoretical analysis provides a way to predict the change in frequency for a certain variation in these parameters. The effect of these parameters is discussed below.

4.1.1 Effect of mass of diaphragm

A change in the mass of the diaphragm introduces a change in the oscillation frequency. It is found that, keeping all the parameters of the oscillator at a constant value, an increase in the mass of the diaphragm decreases the oscillation frequency while a decrease in the mass increases the frequency. This is because the frequency of a spring-mass system is inversely proportional to the square root of the mass. Table 1 shows the values of the oscillation frequencies for a 25% increase and decrease in the lumped mass of the diaphragm.

4.1.2 Effect of seat and vent chamber diameters

A change in the seat chamber diameter or vent chamber diameter also changes the oscillation frequency. The results of the analysis show that the oscillation frequency increases as the diameter of the seat or vent chamber is decreased. Figs. 9 and 10 show the effect of oscillation frequency on the seat chamber and vent chamber diameters.

This effect can be explained by drawing the diaphragm displacement for the entire cycle of operation. Figs. 11 and 12 show the position of the diaphragm for different cross-sectional areas of seat and vent chambers. It is found that the diaphragm travels a greater distance when the diameters of the chambers are increased and hence takes more time for the entire cycle of operation, causing a decrease in frequency.

4.1.3 Effect of spring stiffness

Variation in spring stiffness affects the oscillation frequency. The results of the analysis show that an increase in spring stiffness increases the oscillation frequency. This phenomenon can be explained by observing the diaphragm displacement for springs of different stiffness. Fig. 13 shows the diaphragm displacement for springs of stiffness 30 lb_f/in and 25 lb_f/in. The figures indicate that the diaphragm has displaced more from the seat for a spring having less stiffness and hence the time required for the cycle is more in the case of a less stiff spring. Fig. 14 shows the effect of spring stiffness on the oscillation frequency.

4.1.4 Effect of initial spring force

The effect of initial spring force on the oscillation frequency is shown in Fig. 15. The oscillation frequency is found to decrease as the initial spring force decreases. The initial spring force is equal to the product of the spring stiffness and the initial displacement of the spring. Hence, a decrease in the initial spring force may be viewed as keeping the initial spring displacement as a constant and decreasing the spring stiffness. Since a decrease in the spring stiffness decreases the oscillation frequency, the effect of decreasing initial spring force is to decrease the oscillation frequency.

4.1.5 Effect of output orifice diameter

The theoretical analysis shows that an increase in the output orifice diameter increases the oscillation frequency. Table 2 shows the effect of oscillation frequency on the vent tube geometry for different output orifice diameters. This effect can be explained as follows. When the diameter of the output orifice is decreased, the pressure recovered in the seat chamber is more and causes the diaphragm to move a greater distance from the seat. Thus it introduces an increase in the time required for the operating cycle. Hence the oscillation frequency decreases for a decrease in the output orifice diameter.

4.1.6 Effect of supply pressure

The effect of supply pressures on the oscillation frequency is shown in Table 3. It is found that the oscillation frequency increases as the supply pressure increases.

This phenomenon can be explained as follows. When the supply pressure increases, the diaphragm is displaced a greater distance from the seat due to higher pressure in the seat chamber. But because of this higher pressure recovery, the velocity of the diaphragm movement increases rapidly, reducing the time required for the diaphragm displacement. Hence the total time for the operating cycle decreases and thus increases the frequency of oscillation.

4.2 Experimental Results and Correlation with the Theory

The experimental work carried out gives the variation in the output pressure and the oscillation frequency for vent tubes of different lengths and diameters. The recordings made for different vent tube geometry, supply pressure and spring force are shown in Figs. 16(a) to 16(g). Figs. 16(a), 16(b) and 16(c) show the effect of supply pressure on the oscillation frequency and the output pressure for a constant spring force and a given geometry of vent tube. These figures correspond to supply pressures of 40, 30 and 20 psig for a vent tube of length 8 inches and diameter 5/32 inch and with an initial spring force of 3 lb_f. Figs. 16(d) and 16(e) show the effect of vent tube geometry on the frequency of oscillation and the output pressure. The experimental results show that the oscillation frequency increases as the vent tube diameter increases or as the vent tube length decreases and thus confirms that the oscillation frequency is inversely proportional to the inertance of the vent tube. Figs. 16(f) and 16(g) show the effect of initial spring force on the oscillation frequency and the output pressure. The figures indicate the output pressure fluctuations for a constant supply pressure of 40 psig and for a vent tube of given geometry with the initial spring force of 3 lb_f and 6 lb_f. This experimental result shows that the frequency of oscillation increases with the increase in the initial spring force and thus agrees with the theoretical analysis as shown in Fig. 15. Fig. 17 shows the effect of vent tube geometry on the oscillation frequency for constant supply pressure and initial spring force. The experimental results are in close agreement with the theoretical results obtained for the blocked output under the same operating conditions and are shown in Fig. 18.

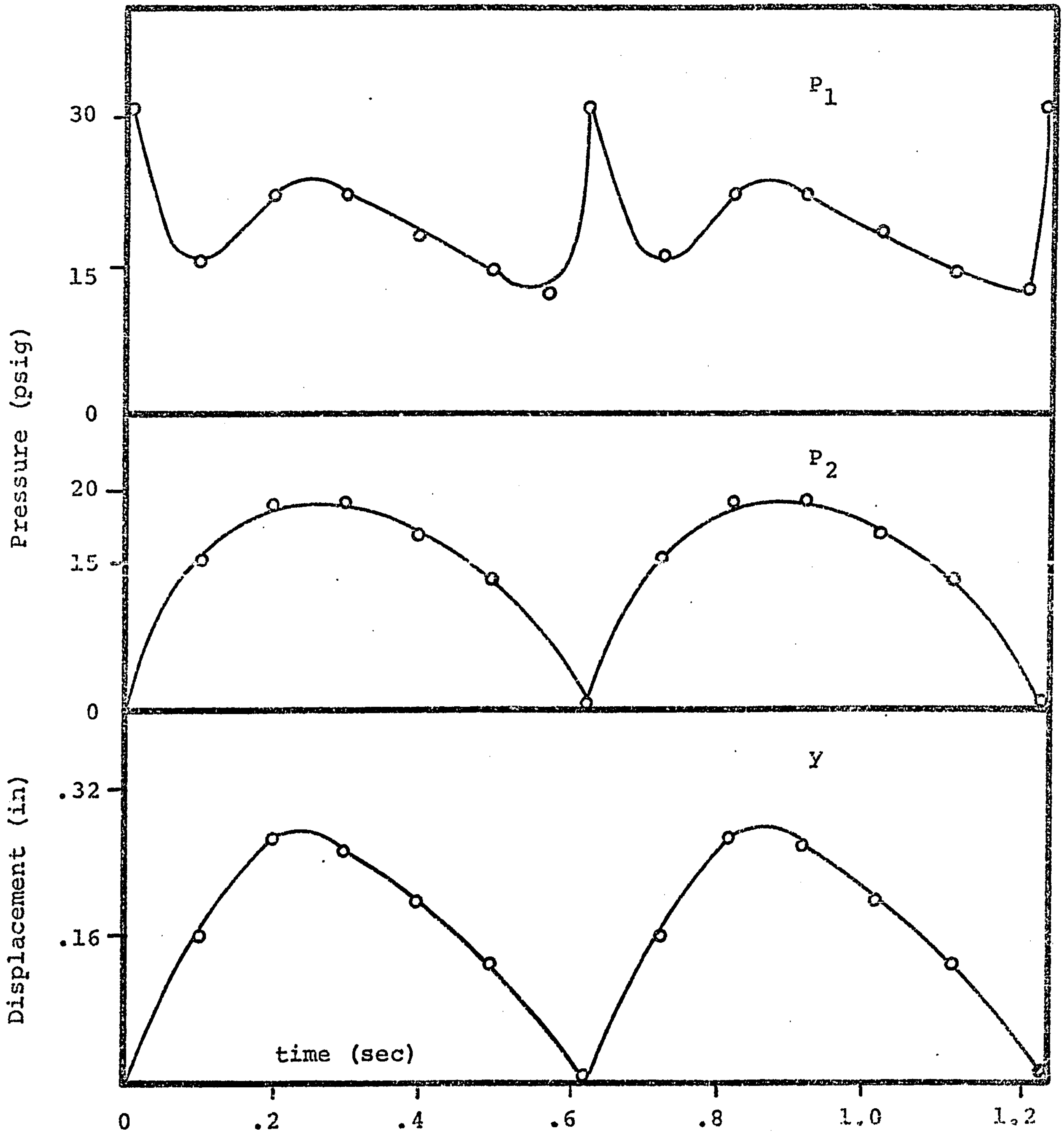

FIG. 5. TYPICAL PRESSURE FLUCTUATIONS IN THE SEAT AND VENT CHAMBER AND THE DIAPHRAGM DISPLACEMENT FOR A VENT TUBE OF 12 INCHES LENGTH AND 5/32 INCH DIAMETER.

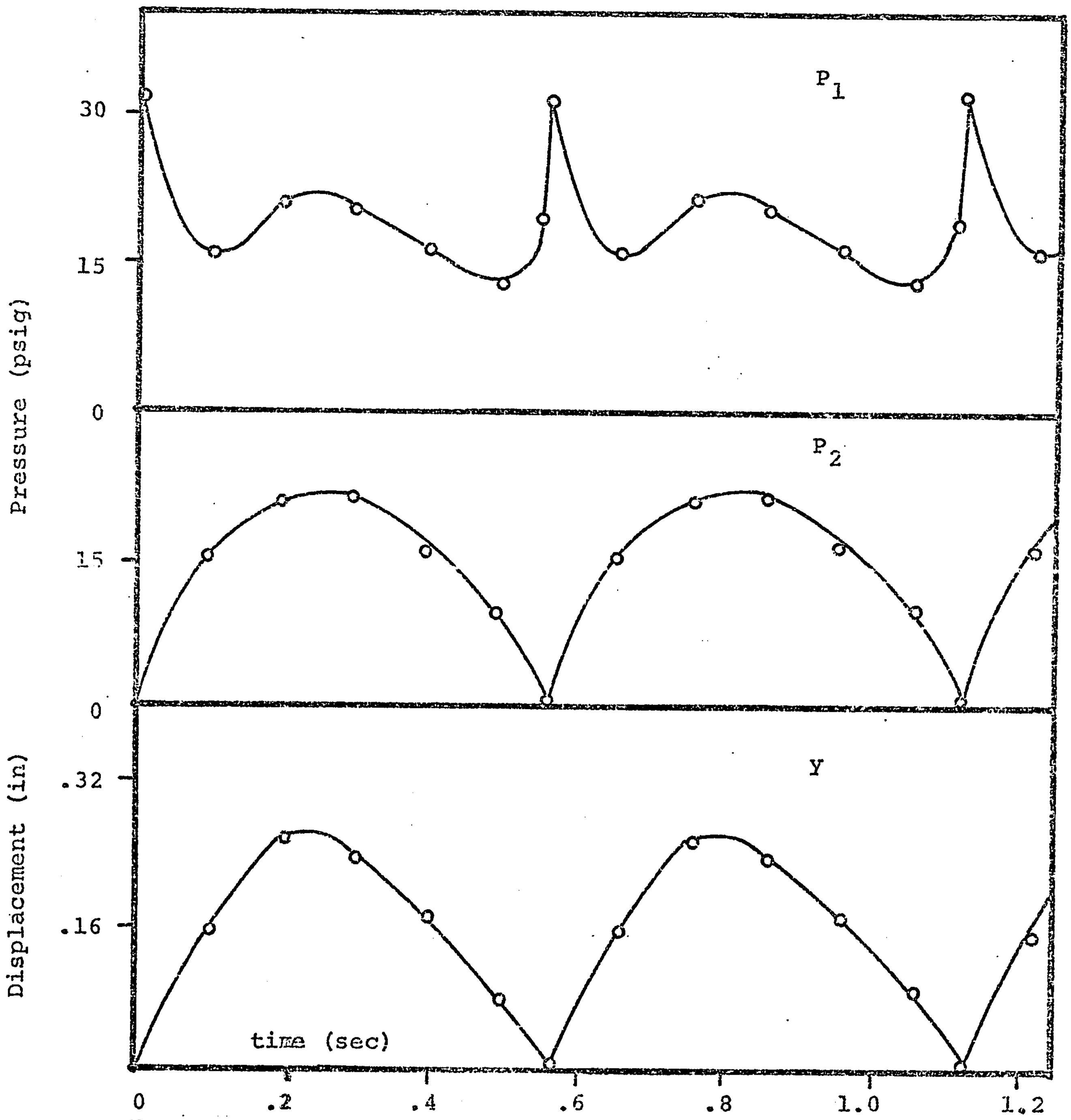

FIG. 6. TYPICAL PRESSURE FLUCTUATIONS IN THE SEAT AND VENT CHAMBER AND THE DIAPHRAGM DISPLACEMENT FOR A VENT TUBE OF 10 INCHES LENGTH AND 5/32 INCH DIAMETER.

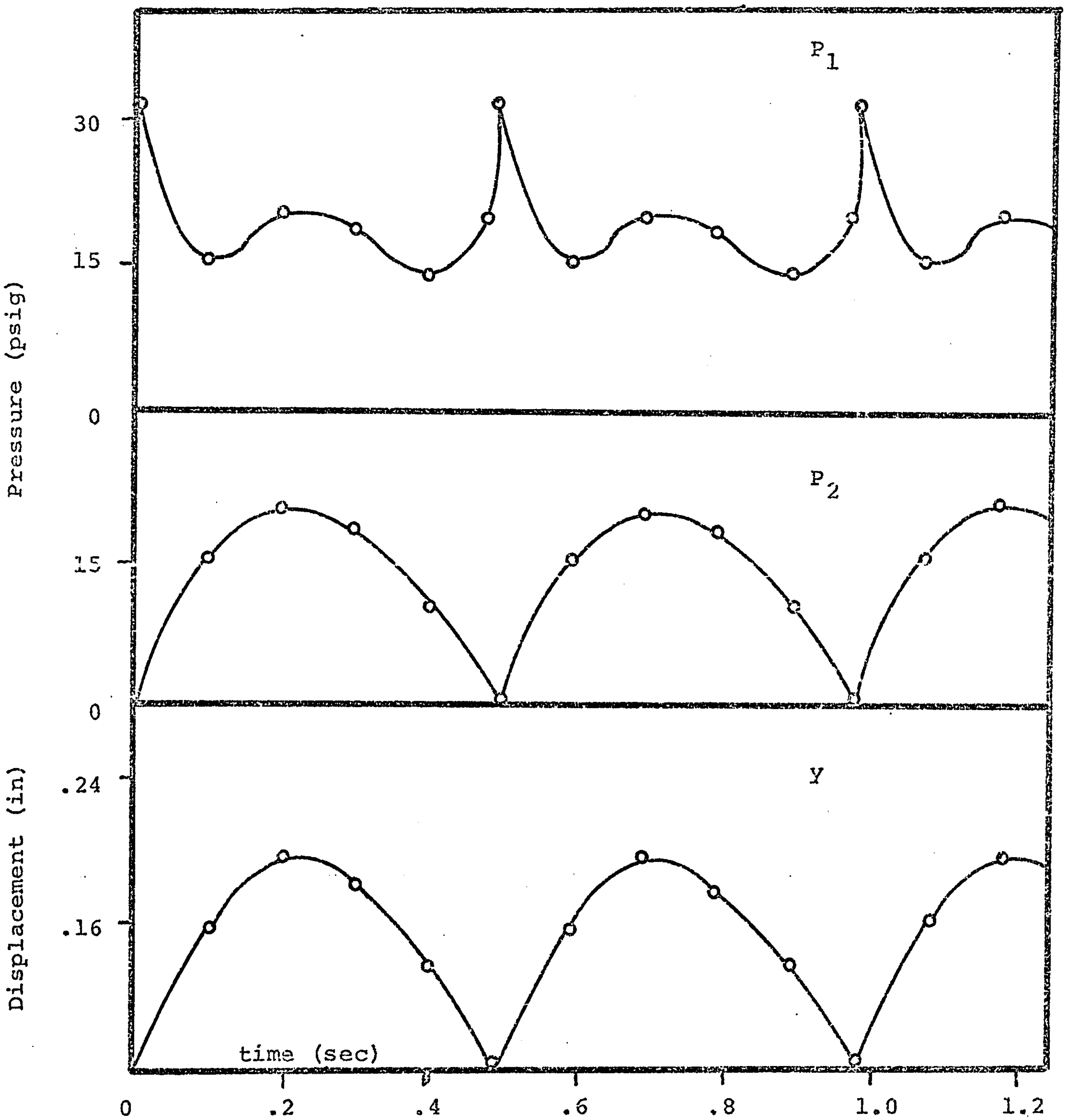

FIG. 7. TYPICAL PRESSURE FLUCTUATIONS IN THE SEAT AND VENT CHAMBER AND THE DIAPHRAGM DISPLACEMENT FOR A VENT TUBE OF 8 INCHES LENGTH AND 5/32 INCH DIAMETER.

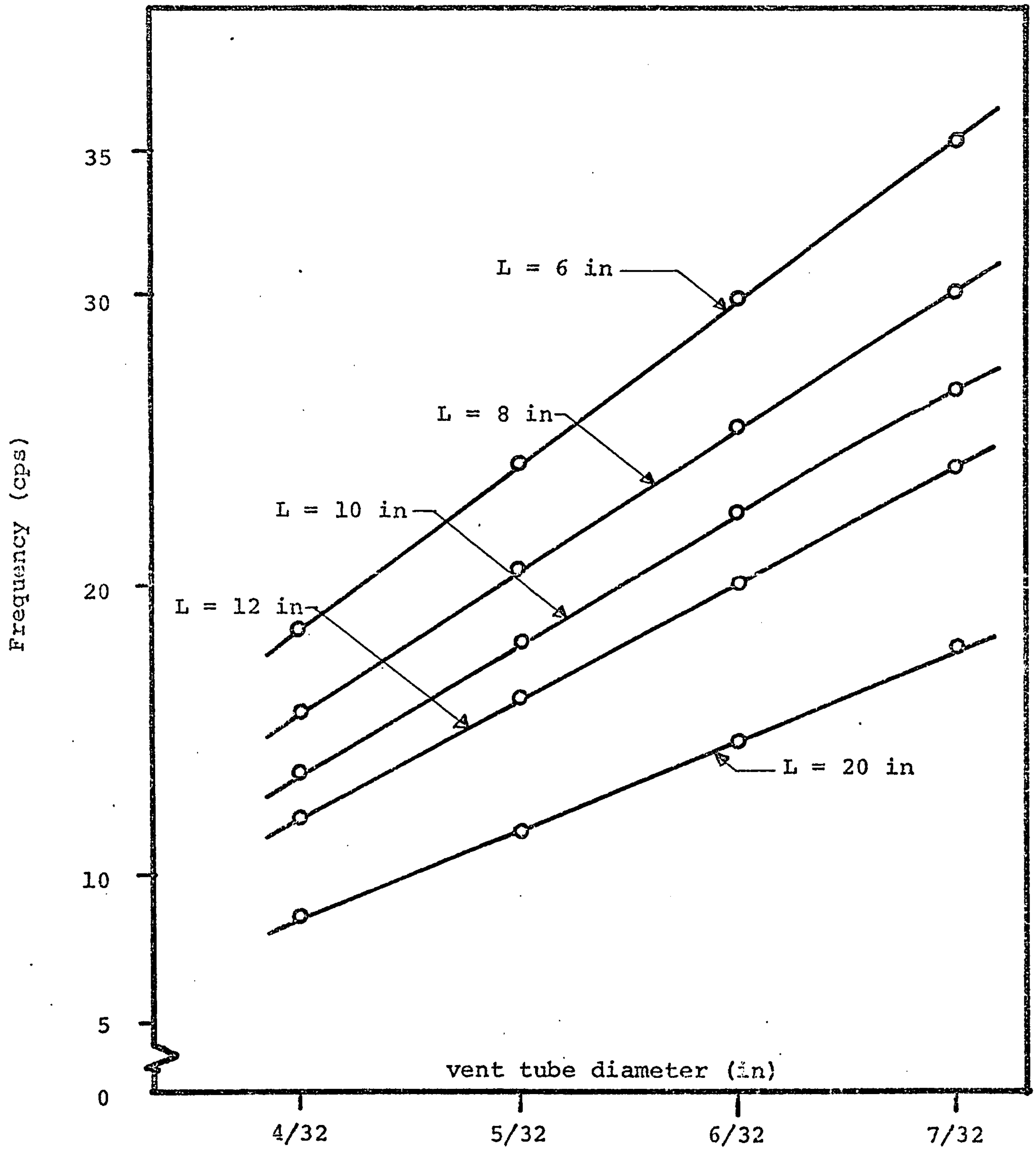

FIG. 8. EFFECT OF VENT TUBE GEOMETRY ON THE OSCILLATION FREQUENCY.

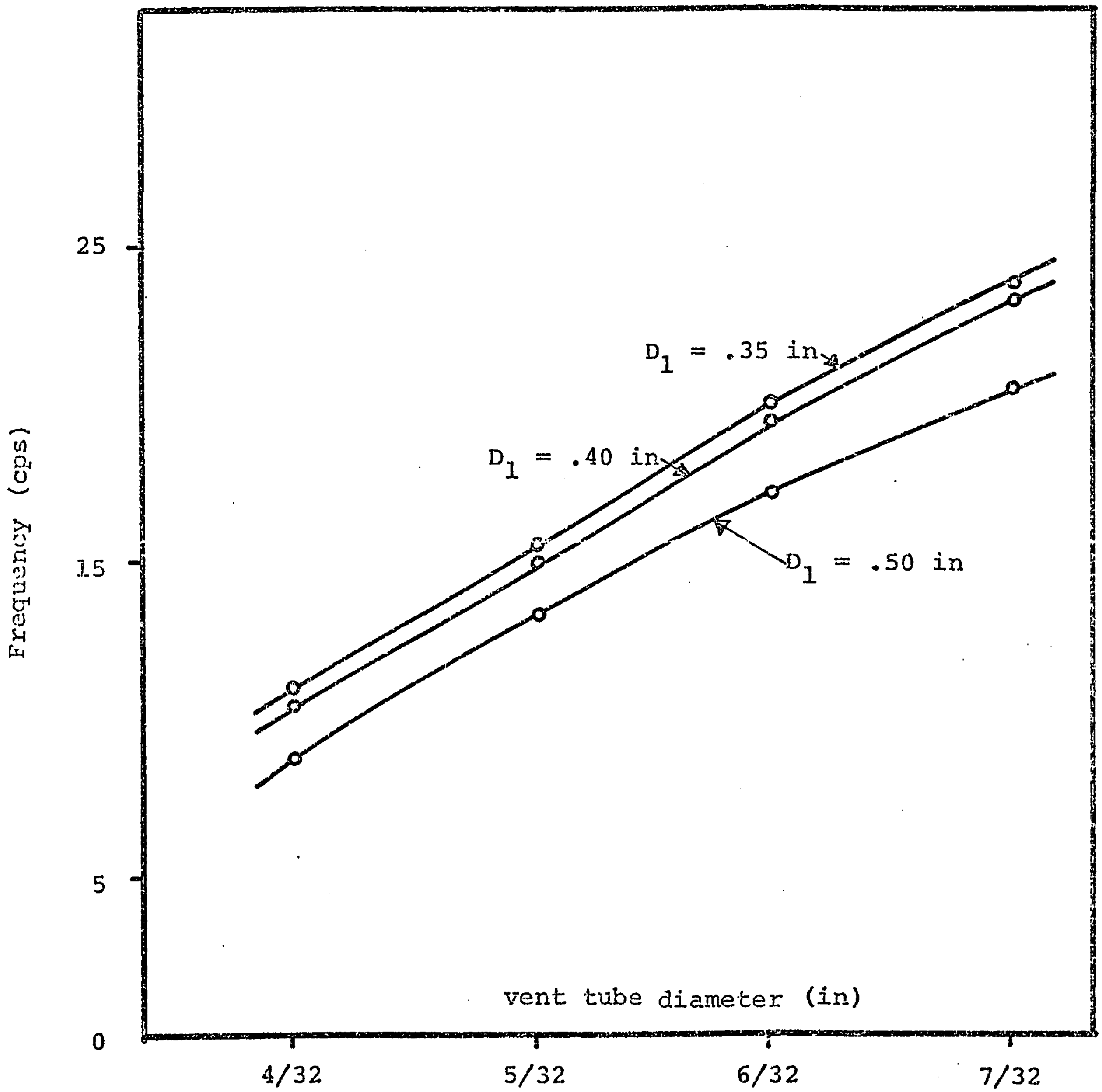

FIG. 9. EFFECT OF SEAT CHAMBER DIAMETER ON THE OSCILLATION FREQUENCY.

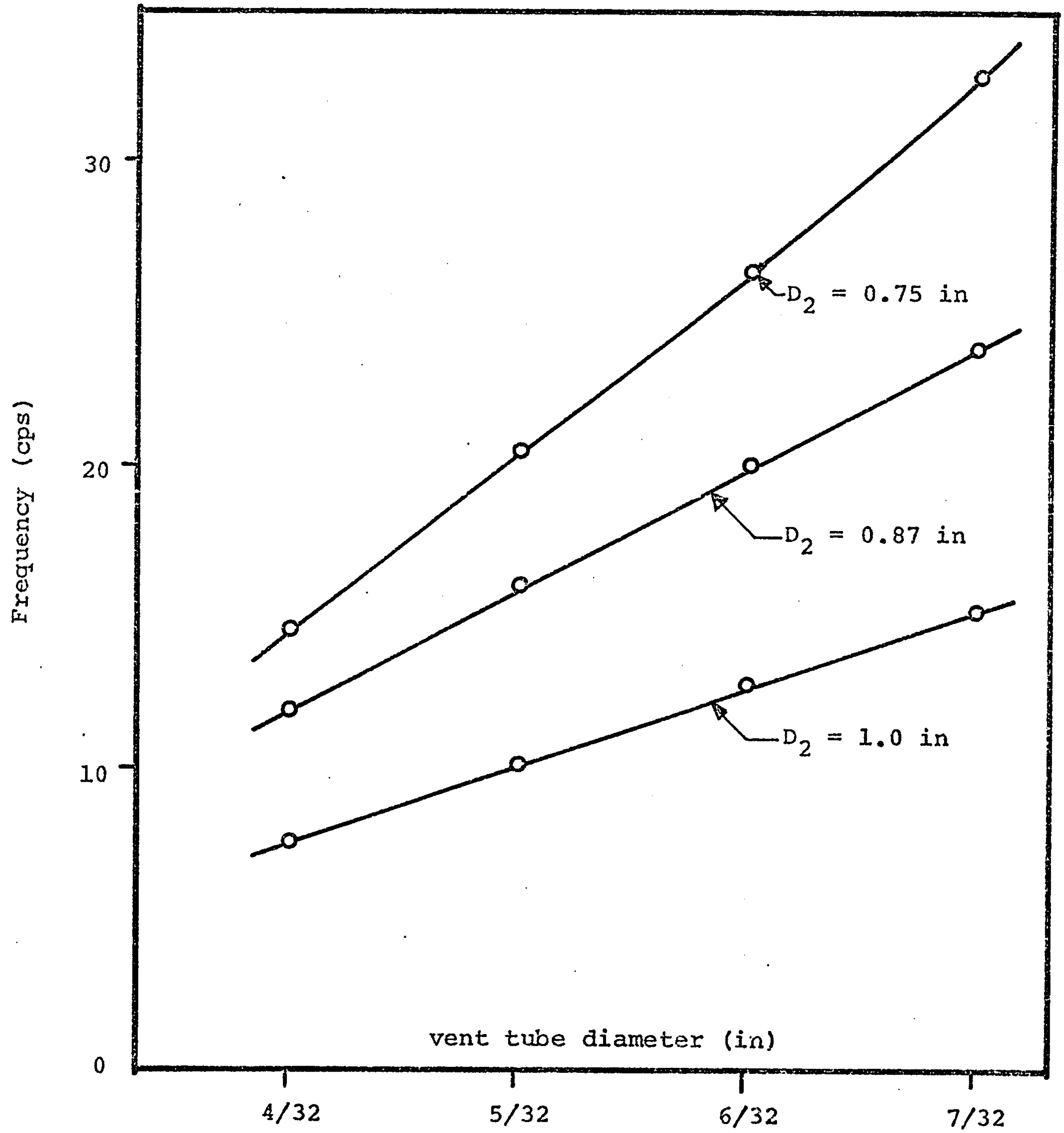

FIG. 10. EFFECT OF VENT CHAMBER DIAMETER ON THE OSCILLATION FREQUENCY.

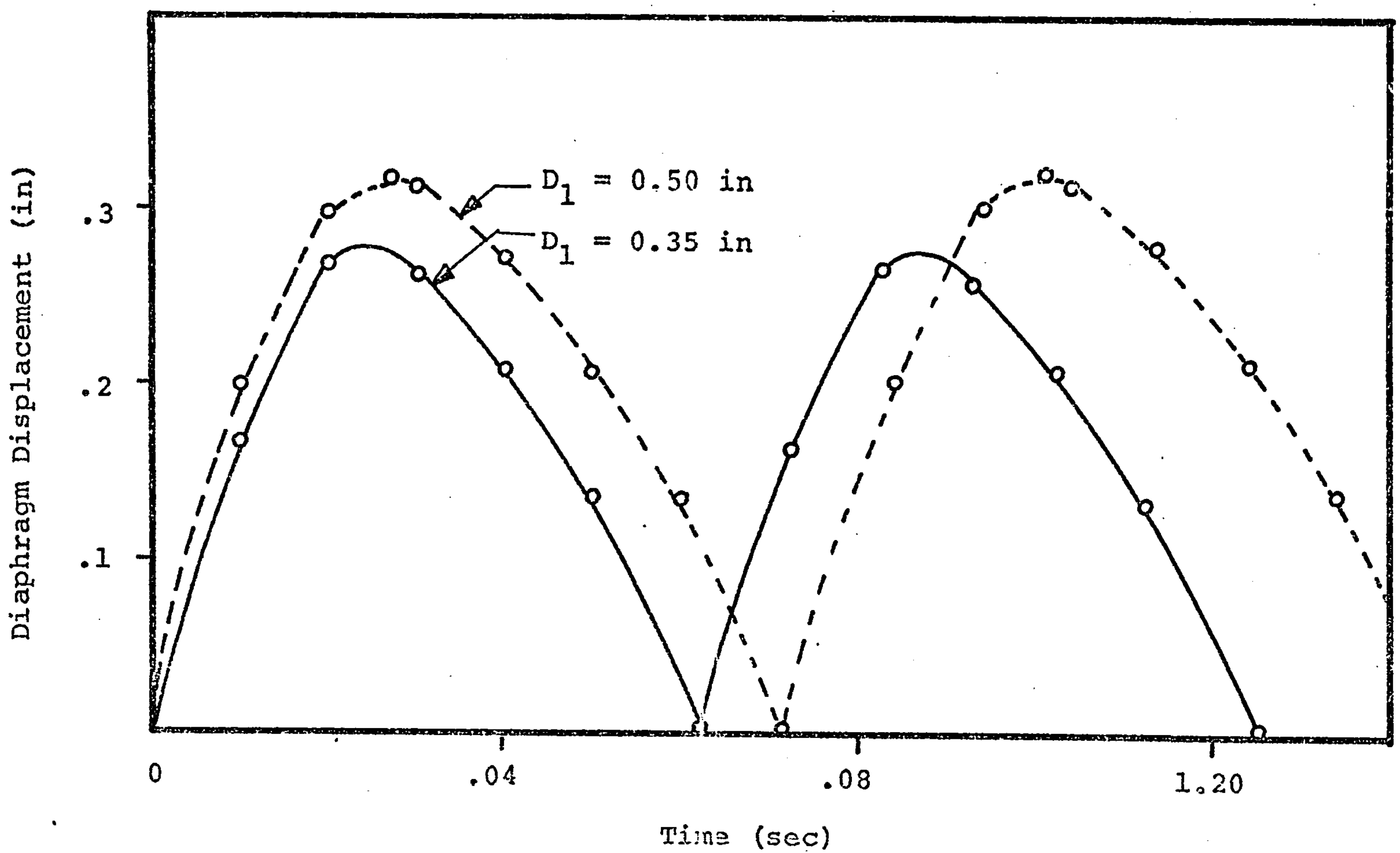

FIG. 11. DIAPHRAGM DISPLACEMENT FOR DIFFERENT SEAT CHAMBER DIAMETER FOR A VENT TUBE OF 12 INCHES LENGTH AND 5/32 INCH DIAMETER.

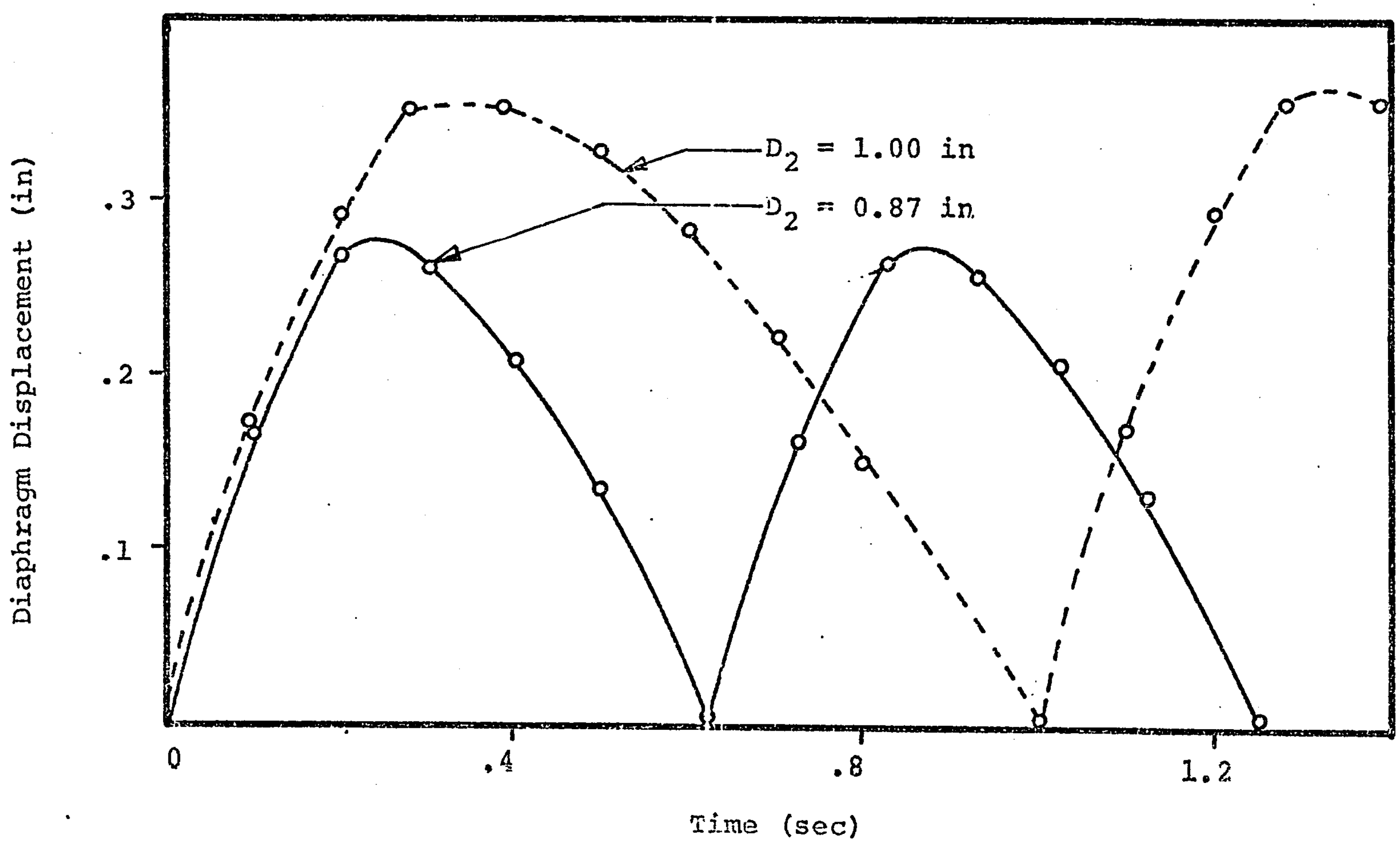

FIG. 12. DIAPHRAGM DISPLACEMENT FOR DIFFERENT VENT CHAMBER DIAMETER FOR A VENT TUBE OF 12 INCHES LENGTH AND 5/32 INCH DIAMETER.

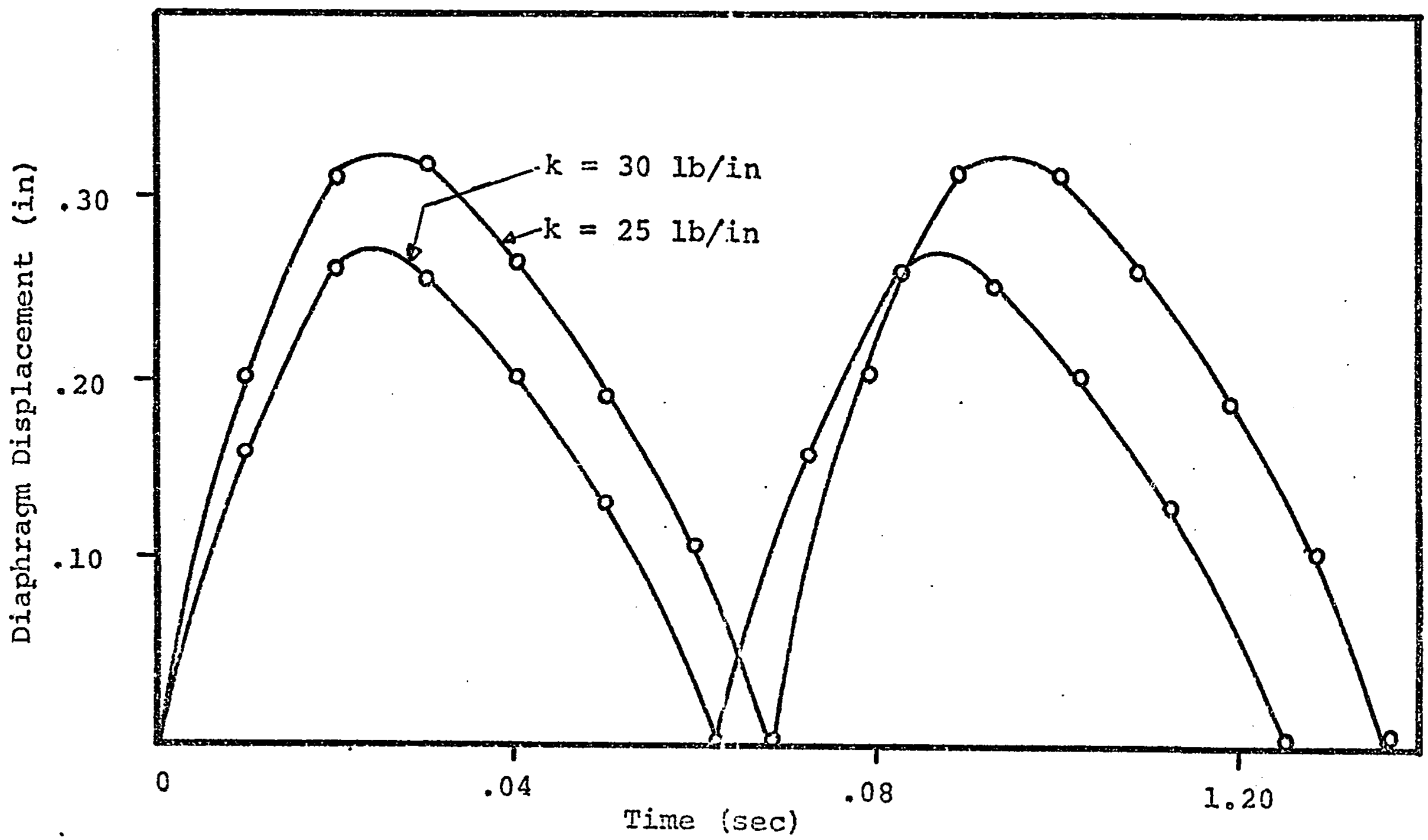

FIG. 13. DIAPHRAGM DISPLACEMENT FOR DIFFERENT SPRING STIFFNESS FOR A VENT TUBE OF 12 INCHES LENGTH AND 5/32 INCH DIAMETER.

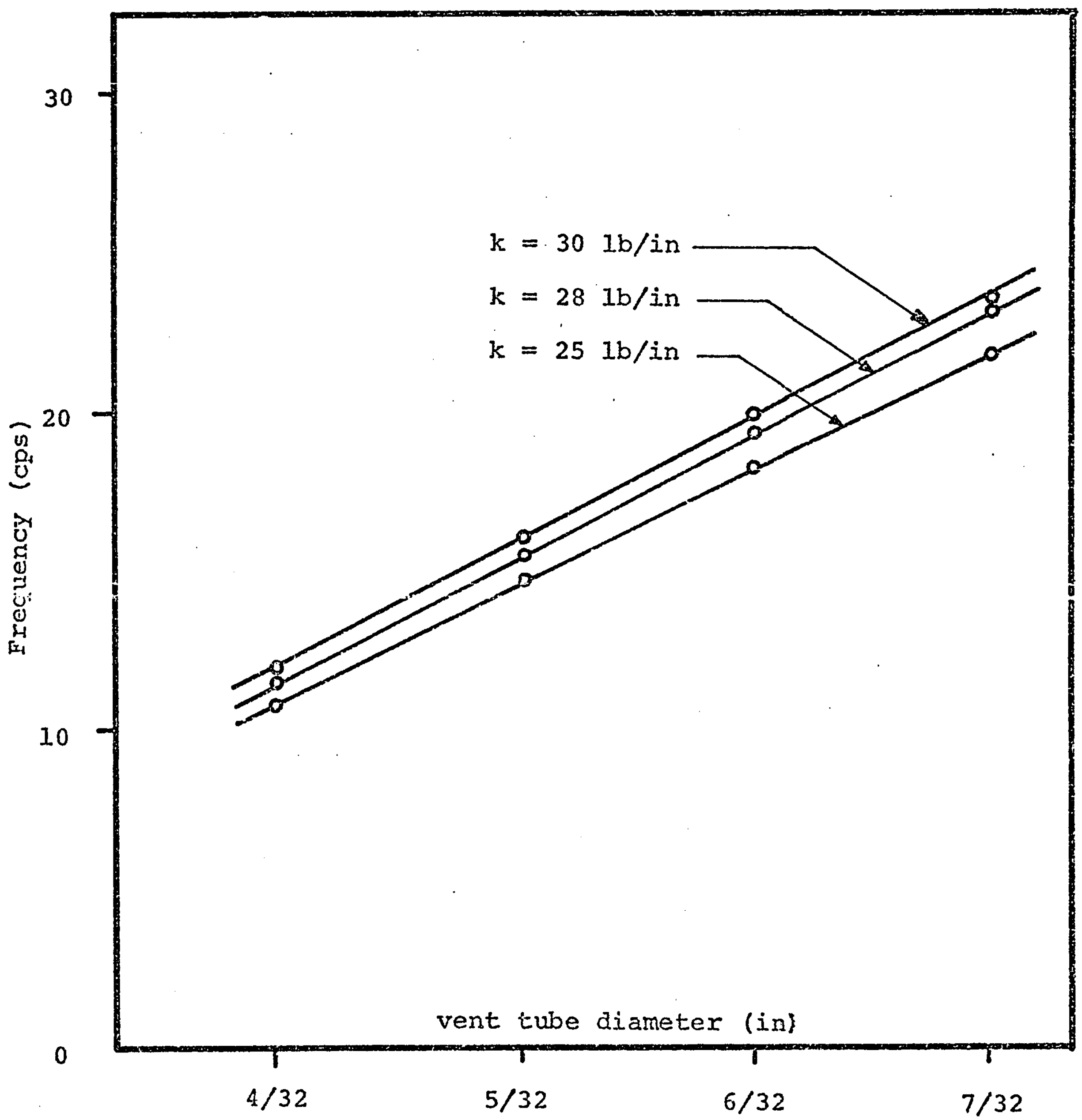

FIG. 14. EFFECT OF SPRING STIFFNESS ON THE OSCILLATION FREQUENCY.

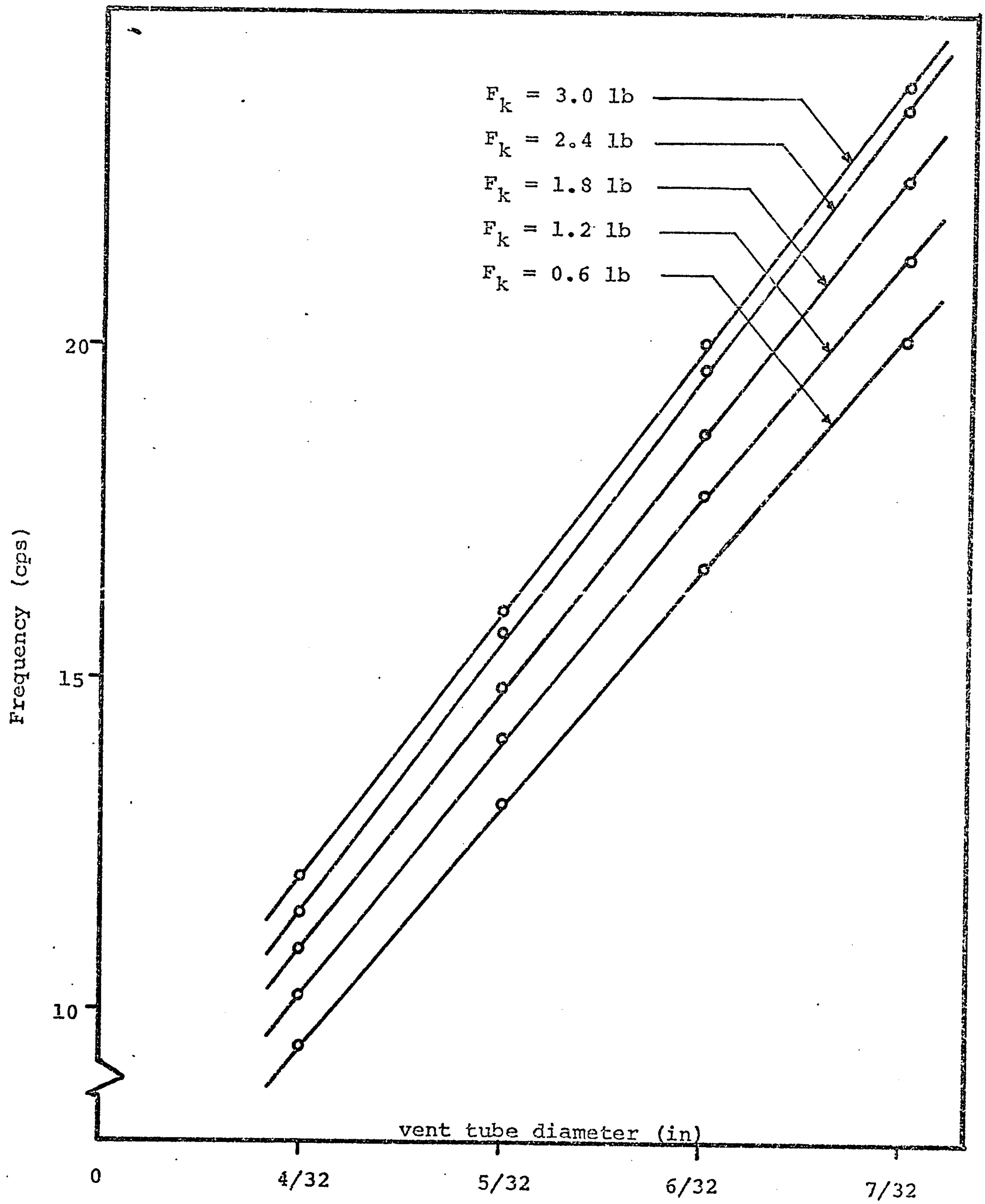

FIG. 15. EFFECT OF INITIAL SPRING FORCE ON THE OSCILLATION FREQUENCY.

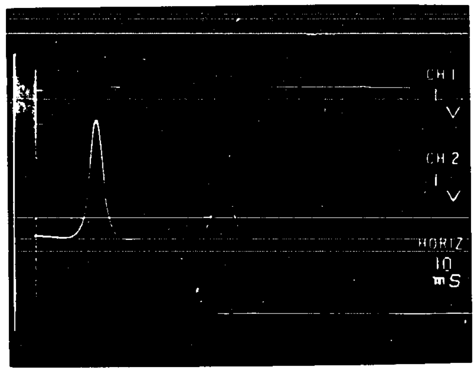

Fig. 16a
P_s = 40 psig
Peak to Peak Pressure = 46.7 psig

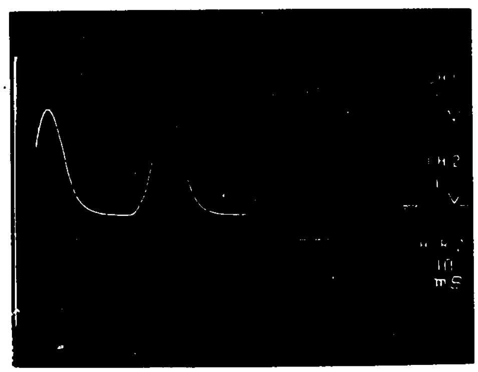

Fig. 16b
P_s = 30 psig
Peak to Peak Pressure = 44 psig

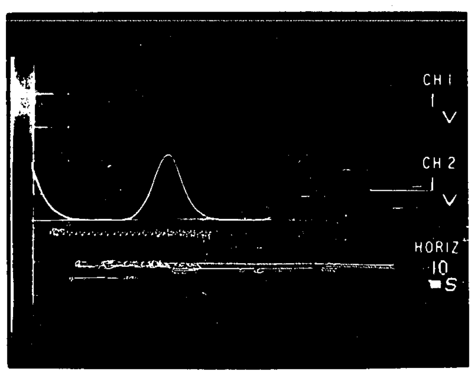

Fig. 16c
P_s = 20 psig
Peak to Peak Pressure = 29.3 psig

Horizontal Line (CH 2) Represents Ambient Pressure Level

TYPICAL OUTPUT PRESSURE WAVEFORMS AT DIFFERENT SUPPLY PRESSURES FOR A VENT TUBE OF 8 INCHES LENGTH AND 5/32 INCH DIAMETER.

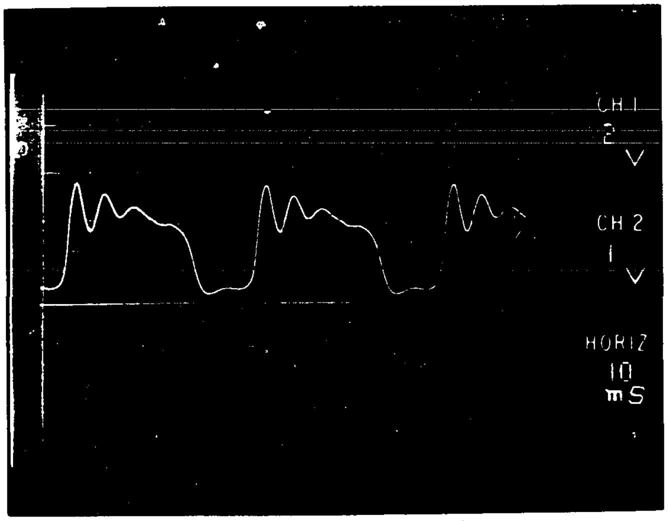

Fig. 16d
P_s = 40 psig
L = 12 inches
Peak to Peak Pressure = 30 psig

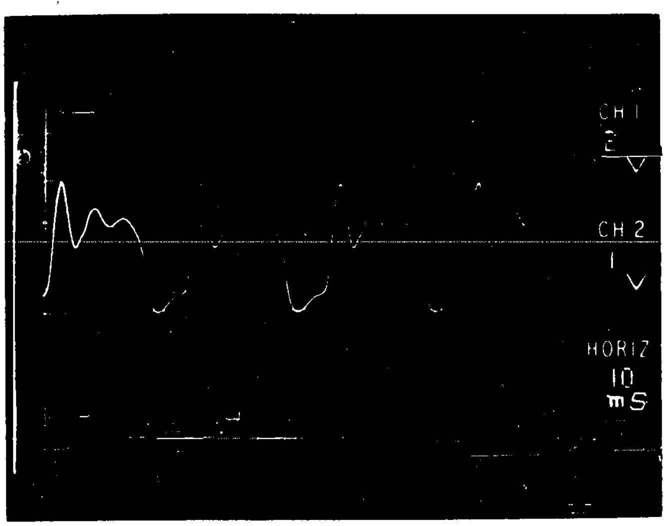

Fig. 16e
P_s = 40 psig
L = 6 inches
Peak to Peak Pressure = 40 psig

Horizontal Line (CH 2) Represents the Ambient Pressure Level

TYPICAL OUTPUT PRESSURE WAVEFORMS FOR A VENT TUBE OF 6/32 INCH DIAMETER.

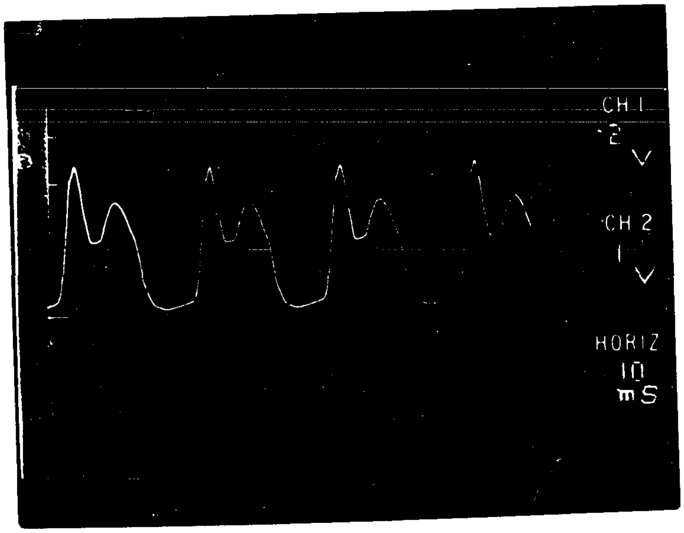

Fig. 16f
P_s = 40 psig
F_k = 30 lb.
Peak to Peak Pressure = 40 psig

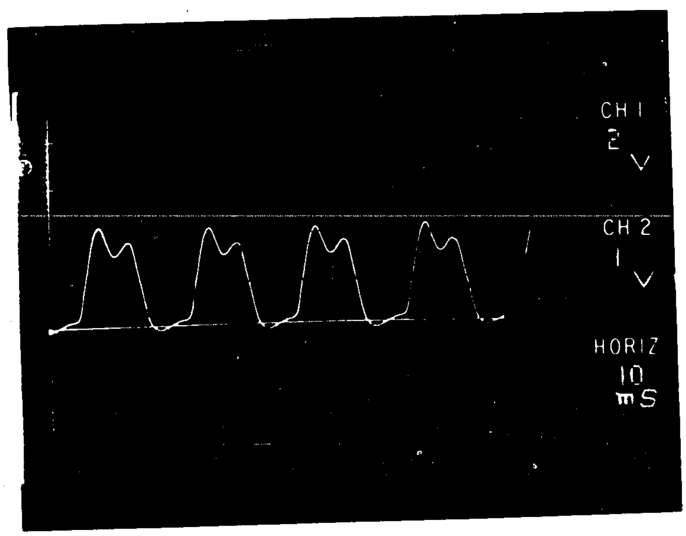

Fig. 16g
P_s = 40 psig
F_k = 60 lb.
Peak to Peak Pressure = 28 psig

Horizontal Line (CH 2) Represents Ambient Pressure Level

TYPICAL OUTPUT PRESSURE WAVEFORMS AT DIFFERENT SPRING FORCES FOR A VENT TUBE OF 8 INCHES LENGTH AND 6/32 INCH DIAMETER.

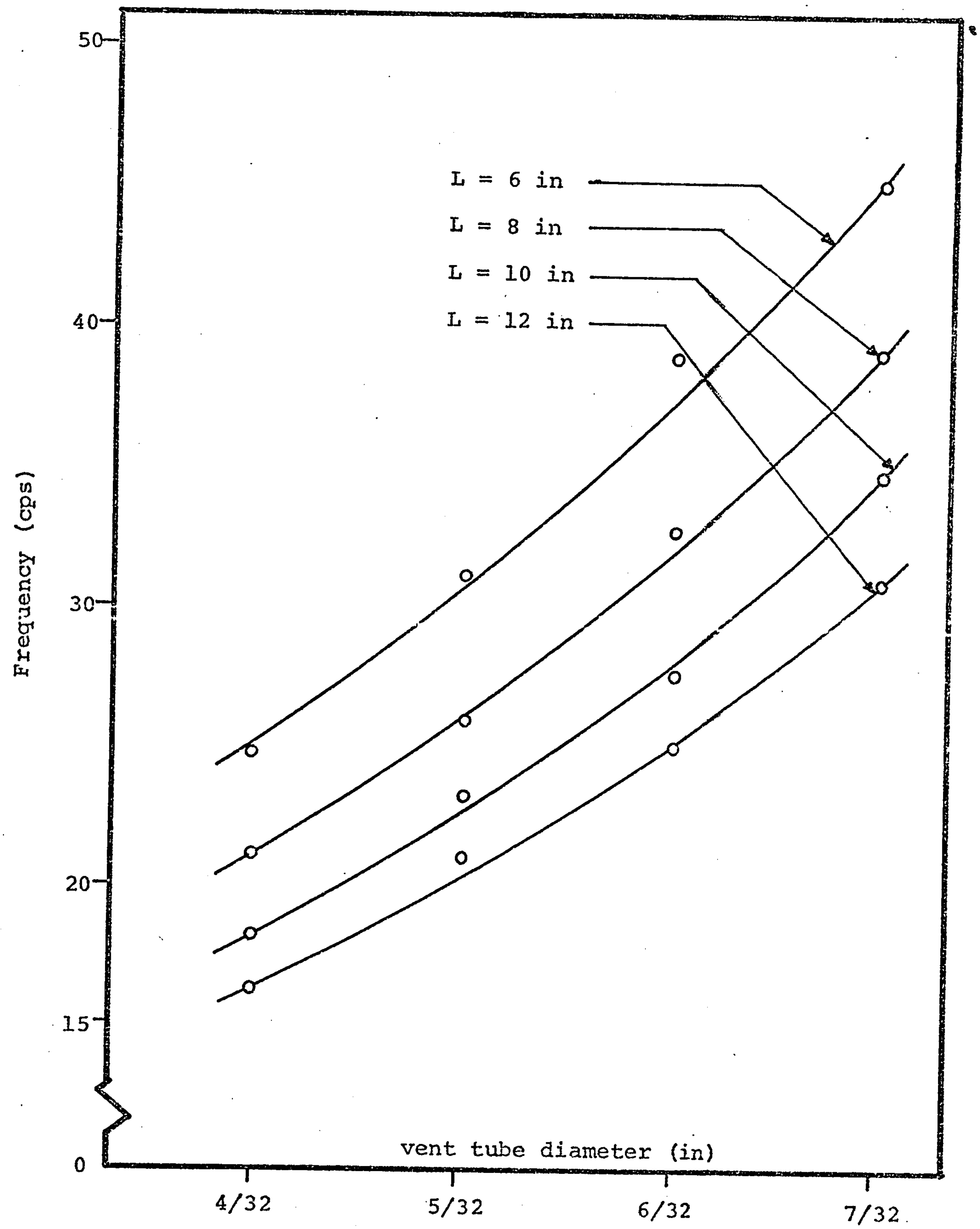

FIG. 17. EXPERIMENTAL RESULTS SHOWING THE EFFECT OF VENT TUBE GEOMETRY FOR A BLOCKED OUTPUT.

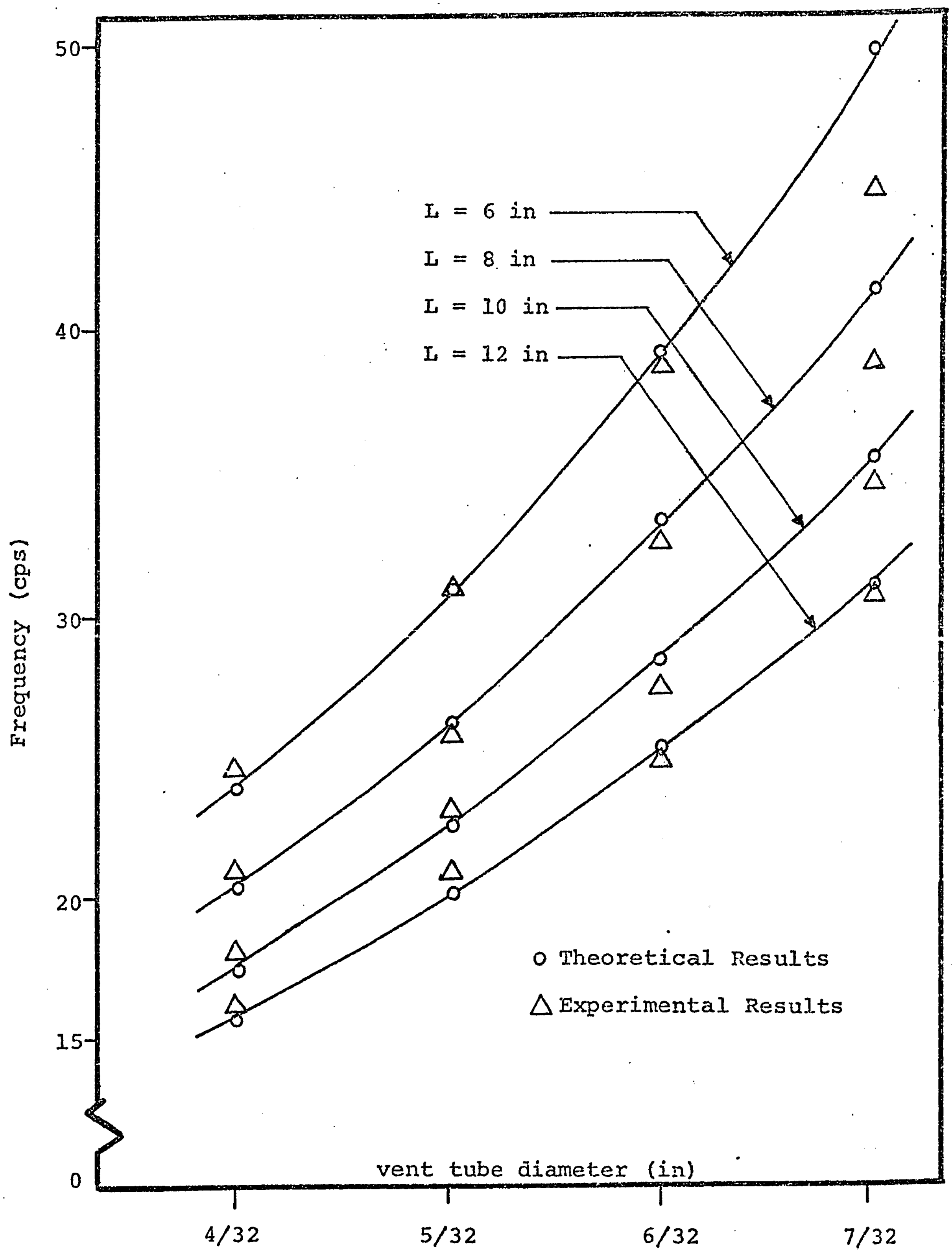

FIG. 18. A COMPARISON BETWEEN THE EXPERIMENTAL RESULTS AND THE THEORETICALLY PREDICTED RESULTS.

TABLE 1

EFFECT OF MASS OF DIAPHRAGM ON THE OSCILLATION FREQUENCY

Mass of Diaphragm (10^{-6} slug)	Diameter of Vent Tube (in)			
	7/32	6/32	5/32	4/32
11.7666	23.84	19.94	15.98	11.92
9.4132	23.90	20.00	16.00	11.93
7.0599	23.96	20.00	16.00	11.95

P_s = 40 psig

L = 12 inches

F_k = 3 lb

TABLE 2

EFFECT OF OUTPUT ORIFICE DIAMETER ON THE OSCILLATION FREQUENCY

Output Orifice Diameter (in)	Diameter of Vent Tube (in)			
	7/32	6/32	5/32	4/32
0.075	23.48	19.65	15.70	11.50
0.100	23.68	19.74	15.81	11.70
0.159	23.90	20.00	16.00	11.93

P_s = 40 psig

L = 12 inches

F_k = 3 lb

TABLE 3

EFFECT OF SUPPLY PRESSURE ON THE

OSCILLATION FREQUENCY

Supply Pressure (psig)	Diameter of Vent Tube (in)			
	7/32	6/32	5/32	4/32
40	23.90	20.00	16.00	11.93
42	24.00	20.04	16.00	11.94
45	24.12	20.09	16.03	11.96

$L = 12$ inches

$F_k = 3$ lb

CHAPTER 5

CONCLUSIONS AND SUGGESTIONS FOR FUTURE STUDIES

5.1 Conclusions

A mathematical model of a diaphragm-type fluid oscillator is presented. The solution of the formulated equations is carried out on a Digital Computer using a Runge-Kutta integration method. The results of the analysis give the pressure fluctuations in the seat and vent chambers and the diaphragm displacement for all instants of time. The theoretical results are in good agreement with the experimental results in predicting the oscillation frequencies for vent tubes of different diameters and lengths.

Based on the theoretical analysis, it can be concluded that the parameters which affect the oscillation frequency are the mass of the diaphragm, the diameter of the vent and seat chambers, the spring stiffness, the supply pressure, the initial spring force, the vent tube length and diameter, and the diameter of the output orifice. It is also concluded that the fluid oscillator operates only due to the inertial effect of the fluid in the vent tube and hence in the absence of the vent tube, the fluid oscillator will not function.

The theory developed could be used as a basis for designing a fluid oscillator to give a specified frequency. The theory can also be extended for designing some possible applications such as a dental irrigator, needle bath shower adaptor, and simple fuel injection system.

5.2 Suggestions for Future Studies

The following suggestions may be outlined to improve the design of the fluid oscillator:

1. The analysis may be done by considering a distributed parameter equivalent of the system.

2. The snap action of the diaphragm may be considered to give closer modelling of the dynamics of diaphragm movement.

3. Experiments may be done on a larger size transparent model to see the various effects inside the oscillator.

4. Provisions may be made in the oscillator for adjusting the spring force and to measure accurately the various pressures to get good experimental results.

REFERENCES

1. S.R. Goldstein, "A differential pulse-length modulated pneumatic servo utilizing floating-flapper-disk switching valves", Journal of Basic Engineering, Trans. ASME, Vol. 90, Series D, No. 2, June 1968, pp. 143-151.

2. A.J. Healey and D.W. Fowler, "Helmholtz Resonator response with F.M. pressure signals", Fourth Cranfield Fluidics Conference, 1970.

3. C.R. Halbach, B.A. Ostap and R.A. Thomas, "A pressure insensitive fluidic temperature sensor", Advances in Fluidics, ASME, 1967, pp. 298-312.

4. M.G. McKinnon, J.N. Wilson and R.W. Besant, "A fluidic digital position sensor", Paper presented at the 23rd Annual Conference of the Instrument Society of America, New York. Paper No. 681945, October 28th-31st, 1968.

5. L.R. Kelley, "A fluidic temperature control using frequency modulation and phase discrimination", Journal of Basic Engineering, Trans. ASME, Vol. 89, Series D, No. 2, June 1967, pp. 341-348.

6. J.R. Frey, J.N. Wilson and R.W. Besant, "Density effects on fluidic feedback oscillators", ASME publication, Paper No. 69-FLCS-39, presented at the Applied Mechanics and Fluids Engineering Conference, Evanston, Ill., June 16th-18th, 1969.

7. J.L. Shearer, A.T. Murphy and H.H. Richardson, "Introduction to System Dynamics", Addison-Wesley Publication Company, Inc., 1967.

8. Gifford White, "Liquid filled pressure gage systems", Statham Instrument Notes No. 7, Statham Instruments, Inc., Los Angeles, California, U.S.A.

9. "Applying Fluidics to Control Systems", course notes, Union College, Editor: Wm. E. Be Vier, July 28th-August 1st, 1969, Section II-A, pp. 8-24.

10. Anthony Ralston, "A first course in numerical analysis", McGraw-Hill Book Company, New York, pp. 191-202.

APPENDIX I

PURE FLUID RESISTANCE

A fluid resistance is an element that causes a pressure drop in a line for a given flow rate. In fluid mechanics it is generally referred to as a restriction. It is always possible to distinguish restrictions by determining the type of flow. Following these conditions, a laminar resistance, a turbulent resistance or a mixed resistance can be defined[9]. If a fluid resistance network has to be established, then it is necessary to know the different equations which have been established as a function of the flow conditions. That is, the pressure drop across the resistor has to be defined as a single valued function of the flow rate.

The fluid oscillator consists of three resistors, namely the supply nozzle, the output orifice and the curtain area. The supply nozzle and the output orifice are turbulent resistances, whereas the flow through the curtain area acts as a mixed resistance. The mixed resistance is defined by large variations of the flow regime as functions of design parameters. The determination of the turbulent resistances can be done using Bernoulli's equation.

Consider the flow through an orifice of cross-sectional area A_o as shown in Fig. A.1. Let P_a and P_b be the pressures at sections (a) and (b). Let A_a and A_b be the

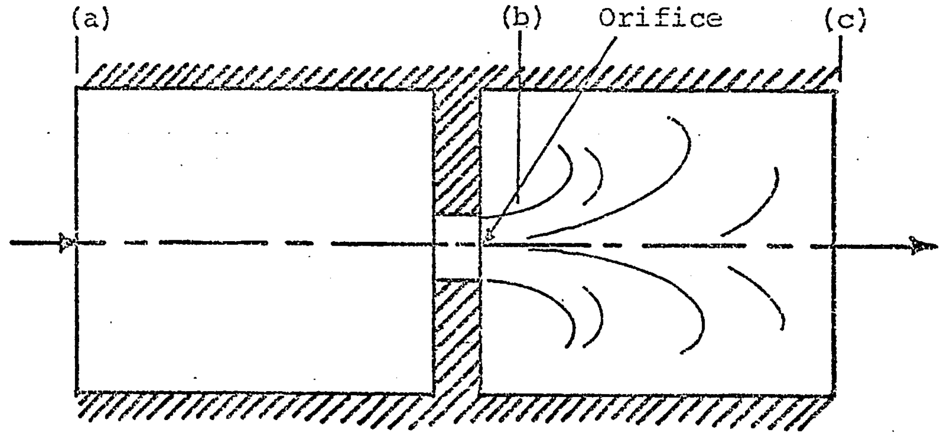

FIG. A.1. FLOW THROUGH AN ORIFICE.

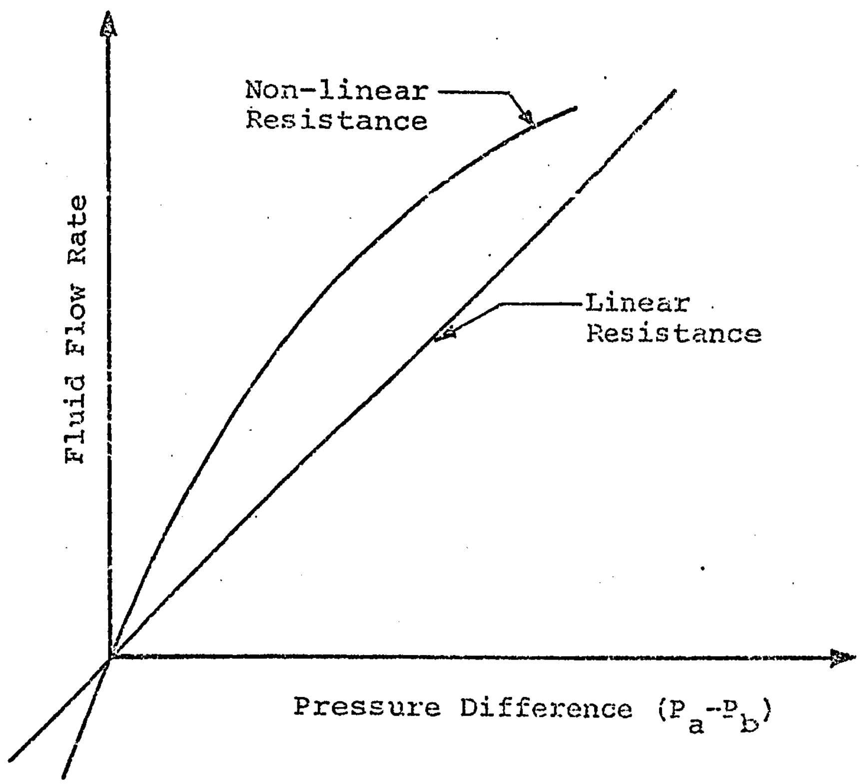

FIG. A.2. CHARACTERISTIC CURVE OF A RESISTANCE.

cross-sectional areas at these sections.

Applying the Bernoulli's equation at sections (a) and (b) gives,

$$H_a + \frac{P_a}{\nu} + \frac{V_a^2}{2g} = H_b + \frac{P_b}{\nu} + \frac{V_b^2}{2g} \qquad \text{(A.1)}$$

where H_a and H_b are the position heads at sections (a) and (b)

V_a and V_b are the velocities at sections (a) and (b)

ν is the specific weight of the fluid

g is the acceleration due to gravity which is equal to 32 ft/sec^2.

Since the position heads at both the sections are the same, the equation (A.1) becomes,

$$\frac{P_a}{\nu} + \frac{V_a^2}{2g} = \frac{P_b}{\nu} + \frac{V_b^2}{2g} \qquad \text{(A.2)}$$

Applying the continuity equation for sections (a) and (b) gives,

$$A_a V_a = A_b V_b \qquad \text{(A.3)}$$

Substituting equation (A.3) in equation (A.2) gives,

$$\frac{P_a}{\nu} + \frac{V_b^2 A_b^2}{2gA_a^2} = \frac{P_b}{\nu} + \frac{V_b^2}{2g} \qquad \text{(A.4)}$$

Assuming there are no losses at the inlet and outlet and simplifying equation (A.4) gives,

$$V_b = \frac{1}{\left[1 - \frac{A_b^2}{A_a^2}\right]^{1/2}} \left[\frac{2}{\rho} (P_a - P_b)\right]^{1/2} \qquad (A.5)$$

where ρ is the density of the fluid.

The volume flow rate through the orifice at the vena contracta is given by

$$Q = C_v A_b V_b \qquad (A.6)$$

where C_v is the velocity coefficient.

Substituting equation (A.5) in equation (A.6) gives,

$$Q = \frac{C_v A_b}{\left[1 - \frac{A_b^2}{A_a^2}\right]^{1/2}} \left[\frac{2}{\rho} (P_a - P_b)\right]^{1/2} \qquad (A.7)$$

$$= C_d A_o \left[\frac{2}{\rho} (P_a - P_b\right]^{1/2} \qquad (A.8)$$

where $$C_d = \frac{C_v C_c}{\left[1 - C_c^{\,2} \frac{A_o^2}{A_a^2}\right]^{1/2}}$$

By definition, the fluid resistance R_f can be written as,

$$R_f = \frac{\Delta P}{Q} = \frac{(P_a - P_b)}{Q} \quad \text{(A.9)}$$

Substituting equation (A.8) in equation (A.9) gives,

$$R_f = \frac{(P_a - P_b)^{1/2}}{C_d A_o (\frac{2}{\rho})^{1/2}} \quad \frac{lb_f\text{-sec}}{in^5} \quad \text{(A.10)}$$

Hence equation (A.10) gives the general formula for a turbulent resistance. Fig. (A.2) shows the consitutive relationships of a turbulent resistance as compared to a linear resistance. Using the formula (A.10), various resistances can be defined as follows.

The resistance of the supply nozzle = $R_n(P_s, P_1)$

$$= \frac{(P_s - P_1)^{1/2}}{C_d A_n (\frac{2}{\rho})^{1/2}} \quad \text{(A.11)}$$

The resistance of the output orifice = $R_o(P_1)$

$$= \frac{P_1^{1/2}}{C_d A_o (\frac{2}{\rho})^{1/2}} \quad \text{(A.12)}$$

The resistance of the curtain area can be derived assuming a square law resistance. The derivation is identical to that of a turbulent resistance.

The resistance of the curtain area = $R_s(P_1, P_2)$

$$= \frac{(P_1 - P_2)^{1/2}}{C_d \pi D y (\frac{2}{\rho})^{1/2}} \quad \text{(A.13)}$$

where D is the diameter of the seat chamber

y is the displacement of the diaphragm measured from the seat.

APPENDIX II

RUNGE-KUTTA METHOD

The system equations consist of three differential equations which have to be solved to get the whole set of solutions. These differential equations can be solved using a Runge-Kutta integration method. The general procedure involved is outlined as follows.

Let $dy/dx = F(x,y)$ (A.14)

Then using the Runge-Kutta method[10], the discrete solution of equation (A.14) is given as,

$$y(n+1) = y(n) + \frac{1}{6}(k_1 + 2k_2 + 2k_3 + k_4)$$

where $k_1 = h.F(x,y)$

$$k_2 = h.F\left(x + \frac{h}{2}, y + \frac{k_1}{2}\right)$$

$$k_3 = h.F\left(x + \frac{h}{2}, y + \frac{k_2}{2}\right)$$

$$k_4 = h.F(x + h, y + k_3)$$

h is the step size equal to $[x(n+1) - x(n)]$.

Considering the system equations, an outline of the procedure involved in the Runge-Kutta integration method for one of the equations is as follows.

Rewriting equation (2.13) gives,

$$\frac{dy}{dt} = \frac{F_m}{m} \tag{A.15}$$

By the Runge-Kutta method, the solution of equation (A.15) is given by

$$y(n + 1) = y(n) + \frac{1}{6}(k_1 + 2k_2 + 2k_3 + k_4)$$

where $k_1 = Dt.\frac{F_m}{m}$

$$k_2 = Dt.\left(\frac{F_m}{m} + \frac{k_1}{2}\right)$$

$$k_3 = Dt.\left(\frac{F_m}{m} + \frac{k_2}{2}\right)$$

$$k_4 = Dt.\left(\frac{F_m}{m} + k_3\right)$$

Dt = step size.

The digital computer program for the whole simulation is provided as follows.

FORTRAN (3.2)/MASTER

```
      PROGRAM FLOUSC
C     SIMULATION OF FLUID OSCILLATOR USING NUMERICAL TECHNIQUE
      EXTERNAL DERIV
      DIMENSION X(3),DV1(5),XOV1(5)
      COMMON XK,YO,YMAX,C3,A1,A2,PS,RCRO,RCR1,CRO,XI
      COMMON XM,PNI,P1,P2,Y,CR1
      READ 30, (DV1(I),I=1,5)
   30 FORMAT (5F10.6)
      READ 40, (XOV1(J),J=1,5)
   40 FORMAT (5F5.3)
C     PS=THE SUPPLY PRESSURE (A CONSTANT)
      PS=40.
C     RHO= THE DENSITY OF THE FLUID (WATER)
      RHO =1.93/(12.**4.)
C     XM= THE MASS OF THE DIAPHRAGM AND THE SPRING RETAINER
      XM=0.0000094132
      PAI=3.141597132
C     CD=THE COEFFICIENT OF DISCHAREGE
      CD=0.62
C     AN= THE CROSSECTIOANAL AREA OF THE NOZZLE
      AN=PAI/4.*0.175*0.175
C     AO=THE CROSSECTIONAL AREA OF THE OUTLET
      AO=PAI/4.*0.159*.159
C     A1 =THE CROSSECTIONAL AREA OF THE SEAT CHAMBER
      A1=PAI/4.*0.35*0.35
C     A2= THE CROSSECTIONAL AREA OF THE VENT CHAMBER
      A2=PAI/4.*(0.87*.87-.5*.5)
C     XK= THE SPRING STIFFNESS
      XK=30.
C     D1= THE DIAMETER OF THE SEAT CHAMBER
      D1=0.35
C     YMAX= MAXIMUM DISPALACEMENT OF THE DIAPHRAGM
      YMAX=0.35
C     YO= INITIAL SPRING DISPLACEMENT
      YO=0.1
      CR1=RHO/(2.*AN*AN)
      CRO=RHO/(2.*(CD*AO)**2.)
      RCR1=SQRT(CR1)
      RCRO=SQRT(CRO)
      C3= RHO/(2.*(CD*PAI*D1)**2.)
      DO 10 J=1,4
C     XOV=THE LENGTH OF THE VENT TUBE
      XOV=XOV1(J)
      DO 10 K=1,3
C     DV= THE DIAMETER OF THE VENT TUBE
      DV=DV1(K)
C     AOV=THE CROSSECTIONAL AREA OF THE OVERFLOW TUBE
      AOV=PAI/4.*DV*DV
      PRINT 60, XOV,DV
   60 FORMAT (//,20X,4HXOV=,F5.3,3HDV=,F10.6)
      XI=RHO*XOV/AOV
      X(1)=0.0
      X(2)=0.0
      X(3)=XK*YO
```

```
FORTRAN (3.2)/MASTER

      T=0.0
      DT=0.00001
      PRINT 2
    2 FORMAT (//,15X,4HTIME,20X,2HP1,20X,2HP2,20X,1HY,20X,4HYDOT)
      DO 10 I=1,80
      CALL RK (X,T,3,DT,100,DERIV)
      PRINT 5, T,P1,P2,Y,X(1)
    5 FORMAT (/,5(10X,F10.5))
   10 CONTINUE
      STOP
      END

         FORTRAN DIAGNOSTIC RESULTS FOR      FLOUSC

NO ERRORS

   FLOUSC     P    00556    C    00042    D    00000
```

FORTRAN (3.2)/MASTER

```
      SUBROUTINE RK(X,T,N,DT,NSTEP,DERIV)
C     X=DEPENDENT VARIABLE
C     T=INDEPENDENT VARIABLE
C     N=NUMBER OF EQUATIONS
C     DT=STEP SIZE
C     DERIV=SUBROTINE TO CALCULATE DERIVATIVE
      DIMENSION X(3)
      DIMENSION XK1(3),XK2(3),XK3(3),XK4(3)
      DO 10 I=1,NSTEP
      CALL DERIV (XK1,X,T)
      DO 20 J=1,3
   20 XK1(J)=XK1(J)*DT
      DO 30 J=1,3
   30 XK2(J)=X(J)+0.5*XK1(J)
      T=T+0.5*DT
      CALL DERIV (XK2,XK2,T)
      DO 40 J=1,3
   40 XK2(J)=XK2(J)*DT
      DO 50 J=1,3
   50 XK3(J)=X(J)+0.5*XK2(J)
      CALL DERIV (XK3,XK3,T)
      DO 60 J=1,3
   60 XK3(J)=XK3(J)*DT
      DO 70 J=1,3
   70 XK4(J)=X(J)+XK3(J)
      T=T+0.5*DT
      CALL DERIV (XK4,XK4,T)
      DO 80 J=1,3
   80 XK4(J) =XK4(J)*DT
      DO 10 J=1,3
   10 X(J)=X(J)+0.1666667*(XK1(J)+2.0*(XK2(J)+XK3(J))+XK4(J))
      RETURN
      END
```

FORTRAN DIAGNOSTIC RESULTS FOR RK

NO ERRORS

RK	P	00362	C	00000	D	00000

```
FORTRAN (3.2)/MASTER
      SUBROUTINE DERIV(DX,X,T)
      DIMENSION DX(3),X(3)
      COMMON XK,YO,YMAX,C3,A1,A2,PS,RCRO,RCR1,CRO,XI
      COMMON XM,PN1,P1,P2,Y,CR1
      YDOT=X(1)
      QI=X(2)
      FK=X(3)
      Y=(FK/XK)-YO
      IF(0.0.LE.Y.AND.YDOT.GT.0.0) GO TO 35
      IF (Y.GE.0.0.AND.YDOT.LT.0.0)   GO TO 30
      IF (Y.GT.0.0.AND.YDOT.EQ.0.0) GO TO 35
      PRINT 26
   26 FORMAT (5H ****)
      Y=0.0
      YDOT=0.0
      QI=0.0
      X(1)=0.0
      X(2)=0.0
      X(3)=XK*YO
      P1=CRO*PS/(CR1+CRO)
      P2=0.0
      DYDOT=(P1*A1-X(3))/XM
      DQI=0.0
      DFK=0.0
      PRINT 60, T,P1,P2,Y,X(1)
   60 FORMAT (/,5(10X,F10.5))
      GO TO 34
   35 IF (Y-YMAX) 30,20,20
   20 Y=YMAX
      YDOT=0.0
   30 CRS=C3/(Y*Y)
      Q1=A1*YDOT
      Q2=A2*YDOT
      QRS=Q2+QI
      Q=QRS+Q1
      QROM=SQRT(PS /CRO)
      XCR1=RCR1*RCR1
      CR1=+XCR1
      XB=2.*CR1*Q/(CRO+CR1)
      XC=(CR1*Q*Q-PS)/(CRO+CR1)
      DET=SQRT(XB*XB-4.*XC)
      QRO1=(-XB+DET)/2.
      QRO2=(-XB-DET)/2.
      IF (QROM-QRO1) 91,92,92
   92 QRO=QRO1
      GO TO 95
   91 CONTINUE
      IF (QROM-QRO2) 95,94,94
   94 QRO=QRO2
   95 CONTINUE
      P1=CRO*ABS(QRO)*QRO
      QR1=Q1+QRO+QRS
      P2=P1-CRS*ABS(QRS)*QRS
      IF (P2) 33,33,44
```

```
FORTRAN (3.2)/MASTER

     33 P2=0.0
     44 CONTINUE
        F1=A1*P1
        F2=A2*P2
        FM=F1+F2-FK
        DYDOT=FM/XM
        IF (Y.EQ.YMAX.AND.DYDOT.GT.0.0) DYDOT=0.0
        DFK=XK*YDOT
        DQI=P2/XI
        X(1)=YDOT
     36 DX(1)=DYDOT
        DX(2)=DQI
        DX(3)=DFK
        RETURN
        END
```

FORTRAN DIAGNOSTIC RESULTS FOR DERIV

```
NO ERRORS
  DERIV      P   00541   C   00042   D   00000
OBJ.LGO
```

APPENDIX III

FLUID OSCILLATOR CONSTANTS

A_1 = 9.6×10^{-2} in^2

A_2 = 0.3982 in^2

A_n = 3.0×10^{-3} in^2

A_o = 1.98×10^{-2} in^2

c_d = 0.62

D_1 = 0.35 in

D_v = 7/32 in, 6/32 in, 5/32 in and 4/32 in

k = 30 lb/in

L = 12 in, 10 in, 8 in and 6 in

m = 9.4132×10^{-6} slug

P_s = 40 psig, 30 psig and 20 psig

y_{max} = 0.35 in

ρ = 9.3×10^{-5} slug/in^3

APPENDIX IV

FLUID MOTION IN THE VENT CHAMBER AND VENT TUBE WHEN THE DIAPHRAGM CLOSES THE CURTAIN AREA

When the diaphragm closes the curtain area, the fluid motion in the vent chamber and vent tube is entirely different from that when the curtain area is open. When the curtain area is closed, both the vent chamber and vent tube act as variable capacitors with considerable rate of change of flow. The equations concerning the motion of the fluid in the vent portion are derived as follows.

A schematic cross-sectional view of the vent chamber and vent tube is shown in Fig. (A.3). Let x and y be the displacement of the fluid in the vent chamber and vent tube at time (t) seconds, measured as shown in the figure. Then dx/dt and dy/dt will be the mean velocity and d^2x/dt^2 and d^2y/dt^2 will be the acceleration of the fluid in the vent chamber and vent tube.

Now consider the control volume as indicated in Fig. (A.3) and apply the principle of conservation of momentum to this control volume.

It gives,

$$P_2A_2 = \frac{d}{dt}\left[\rho A_2 (H - x)\frac{dx}{dt} + \rho A_v L \frac{dy}{dt}\right] \qquad \text{(A.16)}$$

for $0 \leq x \leq H$

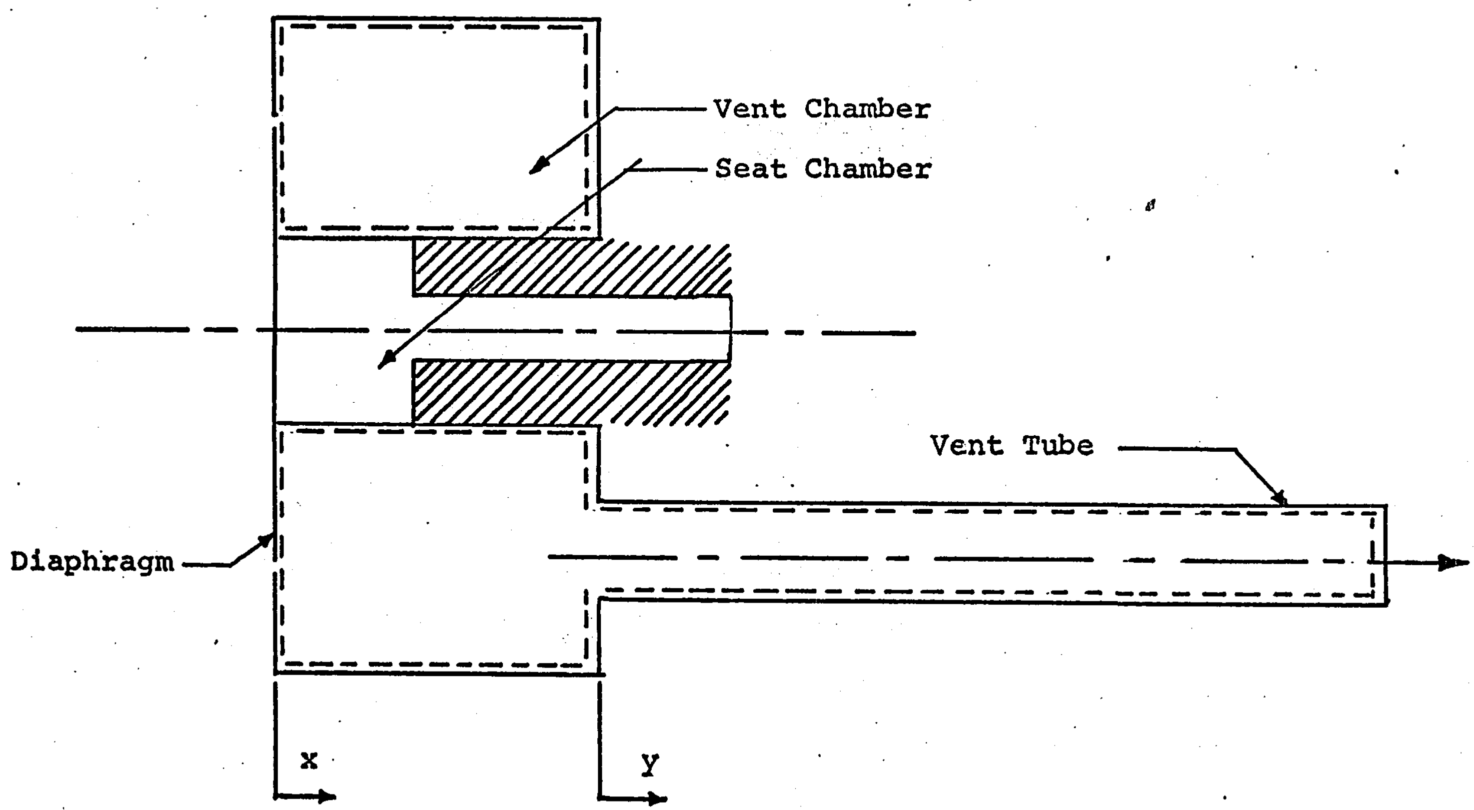

FIG. A.3. SHCEMATIC VIEW OF VENT CHAMBER AND VENT TUBE.

and $$P_2A_v = \frac{d}{dt}\left[\rho A_v(L - y)\frac{dy}{dt}\right] \qquad (A.17)$$

for $0 < y < L$

where H is the length of vent chamber

L is the length of vent tube

A_v is the cross-sectional area of the vent tube

P_2 is the vapour pressure of the fluid.

By simplification and rewriting, equations (A.16) and (A.17) give

$$P_2A_2 = \rho A_2(H - x)\frac{d^2x}{dt^2} - \rho A_2\left(\frac{dx}{dt}\right)^2 + \rho A_v L\frac{d^2y}{dt^2} \qquad (A.18)$$

for $0 \leq x \leq H$

and $$P_2A_v = \rho A_v(L - y)\frac{d^2y}{dt^2} - \rho A_v\left(\frac{dy}{dt}\right)^2 \qquad (A.19)$$

for $0 < y < L$

By continuity equation

$$A_2\frac{dx}{dt} = A_v\frac{dy}{dt} \qquad (A.20)$$

Rewriting equation (A.20) gives,

$$\frac{dy}{dt} = \frac{A_2}{A_v}\frac{dx}{dt} \qquad (A.21)$$

Substituting equation (A.21) in equation (A.18) gives,

$$P_2A_2 = \rho A_2(H - x)\frac{d^2x}{dt^2} - \rho A_2\left(\frac{dx}{dt}\right)^2 + \rho A_2 L\left(\frac{d^2x}{dt^2}\right) \qquad (A.22)$$

$$\text{for} \quad 0 \leq x \leq H$$

Equation (A.22) describes the fluid motion in the vent chamber and vent tube until the fluid is completely drained from the vent chamber. Thereafter, the fluid motion in the vent tube is described by equation (A.19). These two equations are non-linear and the solution is possible only through a digital computer, using a numerical technique. Since these differential equations are second order, the solution requires two initial conditions. For equation (A.22), the first initial condition is the displacement of the fluid, x, at time t equal zero and the second initial condition is the velocity, dx/dt, at t = 0. The initial displacement is zero and the initial velocity can be calculated from the momentum of the fluid when the diaphragm closes the curtain area. Similarly, the initial condition for equation (A.19) is the displacement of the fluid, y, at t = 0 and the velocity, dy/dt, at t = 0. The initial displacement is zero and the initial velocity, dy/dt, can be calculated from the following equation

$$\frac{dy}{dt}\bigg|_{t=0} = \frac{A_2}{A_v}\frac{d\bar{x}}{dt}$$

where $\frac{d\bar{x}}{dt}$ is the velocity of the fluid in the vent chamber just before the chamber is emptied.

The two equations can be solved using the Runge-Kutta method and the results give the position of the interface between the fluid and its saturated vapour. The solution indicates that the fluid in the vent chamber does not drain completely and that it recedes into the chamber after a very short time. The solutions of these equations also show that the time required for this fluid motion is small compared to the operation of the entire cycle. The digital computer program for these equations is provided as follows.

```
FORTRAN (3,2)/MASTER

          PROGRAM VENTUB
          DIMENSION X1(100),Y1(100),Z1(100),Z2(100)
C         P3=SATURATED VAPOUR PRESSURE OF WATER
          P3=-14.5
C         RHO=DENSITY OF WATER
          RHO =1.93/(12.**4.)
          PAI=22./7.
C         DV=DIAMETER OF THE VENT TUBE
          DV=5./32.
C         AOV=CROSS-SECTIONAL AREA OF VENT TUBE
          AOV=PAI*DV*DV/4.
C         A3=VENT CHAMBER DIAMETER
          A3=PAI/4.*(.87*.87-.5*.5)
C         XOV=LENGTH OF VENT TUBE
          XOV=12.
          DT=0.00001
C         H=HEIGHT OF VENT CHAMBER
          H=0.35
          X1(1)=0.0
          Y1(1)=0.0
          Z1(1)=12.3
          N=1
          PRINT 111
      111 FORMAT (//,20X,4HTIME,25X,12HDISPLACEMENT,23X,8HVELOCITY)
       30 T1=DT*Z1(N)
          W1=DT*(P3/RHO+Z1(N)**2)/(H-X1(N)+XOV)
          T2=DT*(Z1(N)+W1/2.)
          W2=DT*(P3/RHO+(Z1(N)+W1/2.)**2)/(H-X1(N)-T1/2.+XOV)
          T3=DT*(Z1(N)+W2/2.)
          W3=DT*(P3/RHO+(Z1(N)+W2/2.)**2)/(H-X1(N)-T2/2.+XOV)
          T4=DT*(Z1(N)+W3)
          W4=DT*(P3/RHO+(Z1(N)+W3)**2)/(H-X1(N)-T3+XOV)
          X1(N+1)=X1(N)+(T1+2.*T2+2.*T3+T4)/6.
          Z1(N+1)=Z1(N)+(W1+2.*W2+2.*W3+W4)/6.
          X11=X1(N+1)
          Z11=Z1(N+1)
          AN=N
          TIME=AN*DT
          PRINT60,TIME,X11,Z11
       60 FORMAT(//,20X,F10.8,20X,E15.5,20X,E15.5)
          IF (X11-H) 100,120,120
      100 CONTINUE
          N=N+1
          GO TO 30
      120 Z2(1)=A3/AOV*Z11
          N=1
          PRINT 110
      110 FORMAT (////, 40X,17HVENT TUBE PORTION)
          PRINT 1111
     1111 FORMAT (//,20X,4HTIME ,25X,12HDISPLACEMENT,23X,8HVELOCITY)
      160 F1=DT*Z2(N)
          G1=DT*(P3/RHO+Z2(N)**2)/(XOV-Y1(N))
          F2=DT*(Z2(N)+G1/2.)
          G2=DT*(P3/RHO+(Z2(N)+G1/2.)**2)/(XOV-Y1(N)-F1/2.)
```

```
FORTRAN (3,2)/MASTER

        F3=DT*(Z2(N)+G2/2.)
        G3=DT*(P3/RHO+(Z2(N)+G2/2.)**2)/(XOV-Y1(N)-F2/2.)
        F4=DT*(Z2(N)+G3)
        G4=DT*(P3/RHO+(Z2(N)+G3)**2)/(XOV-Y1(N)-F3)
        Y1(N+1)=Y1(N)+(F1+2.*F2+2.*F3+F4)/6.
        Z2(N+1)=Z2(N)+(G1+2.*G2+2.*G3+G4)/6.
        Y11=Y1(N+1)
        Z22=Z2(N+1)
        AN=N
        TIME=AN*DT
        PRINT 200, TIME,Y11,Z22
    200 FORMAT(//,20X,F10.8,20X,E15.5,20X,E15.5)
        IF (Y11-XOV) 210,300,300
    210 N=N+1
        GO TO 160
    300 STOP
        END

         FORTRAN DIAGNOSTIC RESULTS FOR      VENTUB

NO ERRORS

   VENTUB      P  02453   C  00000   D  00000
OBJ,LGO
```